Toxicology 303 (2013) 54–71

Contents lists available at SciVerse ScienceDirect

Toxicology

journal homepage: www.elsevier.com/locate/toxicol

Hyaluronic acid-dependent protection in H9C2 cardiomyocytes: A cell model of heart ischemia–reperfusion injury and treatment

Ching-Hsuan Law[a,1], Ji-Min Li[a,1], Hsiu-Chuan Chou[b], Yu-Hua Chen[c], Hong-Lin Chan[a,*]

[a] Institute of Bioinformatics and Structural Biology & Department of Medical Sciences, National Tsing Hua University, Hsinchu, Taiwan
[b] Department of Applied Science, National Hsinchu University of Education, Hsinchu, Taiwan
[c] Department of Biomedical Materials, Material and Chemical Research Laboratories, Industrial Technology Research Institute, Hsinchu, Taiwan

ARTICLE INFO

Article history:
Received 16 October 2012
Received in revised form 8 November 2012
Accepted 9 November 2012
Available online xxx

Keywords:
Hyaluronic acid
Proteomics
Oxidative stress
DIGE
Ischemia–reperfusion injury
Cardiomyocytes

ABSTRACT

Hyaluronic acid (HA), a glycosaminoglycan with high molecular weight, has been reported to promote cell proliferation and serves as an important extracellular matrix component. The aim of this study was to in vitro investigate whether HA is able to reduce reactive oxygen species (ROS)-induced heart ischemia–reperfusion injury and activate the cardiomyocyte's damage surveillance systems. Accordingly, *rattus* cardiomyocyte line, H9C2, was treated with H_2O_2 as a heart ischemia–reperfusion model followed by incubation with low molecular weight hyaluronan (LMW-HA, 100 kDa) or high molecular weight hyaluronan (HMW-HA, 1000 kDa) and proteomic analysis was performed to investigate the physiologic protection of HA in H_2O_2-induced ischemia–reperfusion in cardiomyocyte. Our data demonstrated that HA treatment does protect cardiomyocyte in the ROS-induced ischemia–reperfusion model and the molecular weight of HA is a crucial factor. HMW-HA has been shown to significantly facilitate cell migration and wound healing via cytoskeletal rearrangement. Additionally, 2D-DIGE combined MALDI-TOF/TOF analysis showed that HMW-HA might modulate biosynthetic pathways, cell migration, cell outgrowth and protein folding to stimulate wound healing as well as prevent these ischemia–reperfusion-damaged cardiomyocytes from cell death. To our knowledge, we report for the first time the cell repair mechanism of HMW-HA against ischemia–reperfusion-damage in cardiomyocytes based on cell biology and proteomic analysis.

1. Introduction

In cardiomyocytes, oxygen is mainly reduced by two pathways: one is via the mitochondrial electron transport system, which reduces more than 90% of oxygen to H_2O; the other one is processed by intracellular enzymes to produce ROS (Ferrari et al., 1991). Although endogenous reactive oxygen species (ROS) appear to play important roles in modulating normal cellular processes and the intracellular antioxidant system can balance the effect of ROS under normal conditions, under abnormal condition, the antioxidant mechanism is undermined and ROS-induced tissue damage can take place. Such injury occurs during heart ischemia–reperfusion, where a shortage of blood supply to a region of the heart tissue for a certain period is followed by resumption of blood flow. The severity of the damage from heart ischemia–reperfusion relies on the duration and the degree of the hypoperfusion. Recent studies demonstrated that cardiomyocyte damage induced by heart ischemia–reperfusion has been evidenced to be largely due to the generation of ROS (Venardos and Kaye, 2007; Zhao, 2004; Saini et al., 2004) and Src kinase is a major target to modulate this (Chou et al., 2010). Some other reports also showed that ROS were able to damage the sarcoplasmic reticulum of heart inducing contractile dysfunction and Ca^{2+} release by modifying the structure and function of cardiac proteins (Zima and Blatter, 2006; Saini et al., 2004). This suggested that changes in the redox state of cardiac proteins play an important role in the formation of myocardial ischemia and reperfusion injury.

ROS include several species such as the superoxide (O_2^-), hydroxyl radical (•OH), hydrogen peroxide (H_2O_2) and singlet oxygen (•O). Their related cytotoxicity and formation have been described in several reports (D'Autreaux and Toledano, 2007; Takano et al., 2003; Scandalios, 2002). ROS have been widely

Abbreviations: HA, hyaluronic acid; 1-DE, one-dimensional gel electrophoresis; 2-DE, two-dimensional gel electrophoresis; BSA, bovine serum albumin; CCB, colloidal coomassie blue; CHAPS, 3-[(3-cholamidopropyl)-dimethylammonio]-1-propanesulfonate); ddH_2O, double deionized water; DIGE, differential gel electrophoresis; DTT, dithiothreitol; EDTA, ethylenediaminetetraacetic acid; FCS, fetal calf serum; MALDI-TOF MS, matrix assisted laser desorption ionization-time of flight mass spectrometry; NP-40, Nonidet P-40; SDS, sodium dodecyl sulfate; TFA, trifluoroacetic acid.

* Corresponding author. Tel.: +886 35742476; fax: +886 35715934.
E-mail address: hlchan@life.nthu.edu.tw (H.-L. Chan).

[1] These authors contributed equally to this work.

0300-483X/$ – see front matter © 2012 Elsevier Ireland Ltd. All rights reserved.
http://dx.doi.org/10.1016/j.tox.2012.11.006

reported to play an important role in cell signaling and apoptosis. Among these ROS, H_2O_2 is the dominant form in cells since it is much more stable in comparison with the other ROS (Rhee et al., 2003). In addition, H_2O_2 has been demonstrated to play important roles in reversible protein phosphorylation in numerous cell signaling pathways through mediating the inactivation of PTEN, PTPs and peroxiredoxins by covalent modification of their active site cysteines to form disulfide bonds or Cys-OH. Thus, H_2O_2 has been recognized as a secondary messenger in cells (Barrett et al., 1999; Finkel, 2000; Kwon et al., 2004; Ross et al., 2007; Rhee et al., 2005).

HA, a high molecular weight non-sulfated glycosaminoglycan composed of alternating β-1,4-glucuronic acid and β-1,3-N-acetylglucosamine, is a main extracellular matrix element upon connective tissues. It is initially biosynthesized as large as 1000 kDa disaccharide chains followed by gradually degraded in the extracellular matrix to give intermediate size HA (10–100 kDa) or even small fragments (<1 kDa) (Pauloin et al., 2008). In the view of biological function, HA has been reported to regulate wound healing, cell migration, inflammation and tumor cell metastasis (Toole, 2004). Additionally, HMW-HA has been reported to alleviate benzalkonium chloride- and UVB-induced apoptosis in human corneal epithelial cells (Pauloin et al., 2008, 2009a) and able to speed up wound healing of corneal epithelium in diabetic rats (Yang et al., 2010). Recent studies also demonstrated that HA has an antioxidant activity toward ROS (Young and Woodside, 2001) and was susceptible to be degraded into smaller molecular weight fractions by ROS to compensate the oxidative damage of cells (McCord, 1974).

Proteomics is a tool to rapidly distinguish protein expression alterations across different conditions. 2-DE is presently a crucial method in proteomics to profile thousands of proteins within trace amount of biological samples as well as plays a complementary role to LC/MS-based proteomic analysis (Timms and Cramer, 2008). However, reliable quantitative comparisons across gels and gel-to-gel variations remain the crucial challenge in 2-DE analysis. A significant improvement for the gel-based protein quantification and detection was achieved by the introduction of 2D-DIGE, which can co-detect numerous samples in the same 2-DE. This advance minimizes gel-to-gel variations and allows comparing the relative amount of protein spots across different gels by using an internal fluorescent standard run in all of gels. Moreover, 2D-DIGE technique has the advantages of a higher sensitivity, broader dynamic range and greater reproducibility than traditional 2-DE (Timms and Cramer, 2008). This inventive technology relies on the pre-labeling of protein samples with fluorescent dyes (Cy2, Cy3 and Cy5) before electrophoresis. Each dye has a distinct fluorescent wavelength, allowing multiple samples with an internal standard to be concurrently separated in the same gel. The internal standard, which is a pool of an equal amount of the protein samples, provides accurate normalization results and increase statistical confidence in relative quantification across gels (Huang et al., 2010; Lai et al., 2010; Chou et al., 2010; Chan et al., 2005, 2006; Hung et al., 2011; Chen et al., 2011a).

During heart ischemia–reperfusion injury, the antioxidant defence system is undermined and excess ROS-induced damage to the tissue can take place. Thus, ROS scavengers were long-term tested to alleviate the disease (Martin et al., 2001; Pucheu et al., 1996). Due to the antioxidant potency, wound healing ability and biocompatibility of HA, this study is to assess the HA's antioxidant capacity on heart ischemia–reperfusion injury as well as the effect of HA's molecular weight and concentration on curing heart ischemia–reperfusion injury. In present study, we examined the protective ability of LMW-HA (100 kDa) and HMW-HA (1000 kDa) in ischemia–reperfused rat cardiomyocytes by performing biological assays such as cell viability, wound healing and apoptotic assay. Additionally, proteomic analysis can globally investigate the cellular proteins in response to environmental stimulations. Thus, the proteomic strategy in this study is suitable to evaluate the effects of HA on ischemia–reperfused cardiomyocytes as well as to understand how the HA suppress ischemia–reperfused injury.

2. Materials and methods

2.1. Chemicals and reagents

Generic chemicals were purchased from Sigma–Aldrich (St. Louis, USA), while reagents for 2D-DIGE were purchased from GE Healthcare (Uppsala, Sweden). All primary antibodies were purchased from Genetex (Hsinchu, Taiwan) and anti-mouse and anti-rabbit secondary antibodies were purchased from GE Healthcare (Uppsala, Sweden). All the chemicals and biochemicals used in this study were of analytical grade. The LMW-HA and HMW-HA used in this study were both medical grade (listed in European Pharmacopeia) and purchased from Shiseido Co. (Tokyo, Japan). These HAs contain less than 1% protein content and less than 0.0003 IU/mg bacterial endotoxins. All the chemicals and biochemicals used in this study were of analytical grade.

2.2. Cell lines and cell cultures

The rat cardiomyocyte cell line H9C2 was purchased from the American Type Culture Collection (ATCC) (Manassas, VA) and was maintained in Dulbecco's modified Eagle's medium (DMEM) supplemented with 10% (v/v) FCS, L-glutamine (2 mM), streptomycin (100 μg/mL) and penicillin (100 IU/mL) (all from Gibco-Invitrogen Corp., UK). All cells were incubated in a humidified incubator at 37 °C and 5% CO_2. Cells were passaged at 80% confluence by trypsinization according to standard procedures. Cells cultured in normal growth medium at ~80% confluence were treated with indicated concentrations of H_2O_2. For HA protection, H9C2 cells at ~80% confluence were pre-treated with HA for 30 min prior to treatment with H_2O_2 or vehicle (PBS) for 30 min.

2.3. MTT cell viability assay

H9C2 cells growing exponentially were trypsinized and counted using a hemocytometer. Cells in triplicate wells were seeded at a density of 5000 cells per well into 96-well plates. After washing with PBS three times, the H9C2 cells were transiently treated with indicated concentrations of either HMW-HA (1000 kDa) or LMW-HA (100 kDa) for 30 min or left untreated followed by incubation in serum-free medium containing indicated concentrations of H_2O_2 for 24 h. DMSO treatment groups were served as a negative control. The detail MTT procedure has been described in our previous publication (Chou et al., 2012).

2.4. Scratch wound healing assay

Exponentially growing H9C2 cells were trypsinized and seeded at a density of 200,000 cells per well into 12-well plates for 24 h incubation (~90% confluence). The scratch wounds were made by a sterile 10 μL pipette tip through a pre-marked line. After removal of the resulting debris from five lineal scratches, H9C2 monolayer was subsequently rinsed three times with PBS followed by incubated with PBS containing indicated concentrations of HA for 30 min. After rinsed with PBS, cell were further incubated in 400 μm H_2O_2 for 24 h and rinsed three times with PBS. The wound areas were displayed by taking images just above the interchanges between scratched wound areas and pre-marked lines.

2.5. Sample preparation and 2D-DIGE-based proteomic analysis

The detail experimental procedures have been described in our previous publications (Lai et al., 2010). Briefly, H9C2 cells in normal growth medium at ~80% confluence were used for proteomic analysis. For total cellular protein analysis, cells with various treatments were washed in chilled 0.5 × PBS and scraped in 2-DE lysis buffer containing 4% (w/v) CHAPS, 7 M urea, 2 M thiourea, 10 mM Tris–HCl, pH 8.3, 1 mM EDTA. Lysates were homogenized by passage through a 25-gauge needle 10 times, insoluble material was removed by centrifugation at 13,000 rpm for 30 min at 4 °C, and protein concentrations were determined by using Coomassie Protein Assay Reagent (BioRad). Before performing 2D-DIGE, protein samples were labeled with N-hydroxy succinimidyl ester-derivatives of the cyanine dyes Cy2, Cy3 and Cy5 following the protocol described previously (Wu et al., 2012). Briefly, 150 μg of protein sample was minimally labeled with 375 pmol of either Cy3 or Cy5 for comparison on the same 2-DE. To facilitate image matching and cross-gel statistical comparison, a pool of all samples was also prepared and labeled with Cy2 at a molar ratio of 2.5 pmol Cy2 per μg of protein as an internal standard for all gels. Thus, the triplicate samples and the internal standard could be run and quantify on multiple 2-DE. The labeling reactions were performed in the dark on ice for 30 min and then quenched with a 20-fold molar ratio excess of free L-lysine to dye for 10 min. The differentially Cy3- and Cy5-labeled samples were then mixed with the Cy2-labeled internal standard and reduced with dithiothreitol for 10 min. IPG buffer, pH 3–10 nonlinear

(2%, v/v, GE Healthcare) was added and the final volume was adjusted to 450 μL with 2D-lysis buffer for rehydration. The rehydration process was performed with immobilized non-linear pH gradient (IPG) strips (pH 3–10, 24 cm) which were later rehydrated by CyDye-labeled samples in the dark at room temperature overnight (at least 12 h). Isoelectric focusing was then performed using a Multiphor II apparatus (GE Healthcare) for a total of 62.5 kV-h at 20 °C. Strips were equilibrated in 6 M urea, 30% (v/v) glycerol, 1% SDS (w/v), 100 mM Tris–HCl (pH 8.8), 65 mM dithiothreitol for 15 min and then in the same buffer containing 240 mM iodoacetamide for another 15 min. The equilibrated IPG strips were transferred onto 26 cm × 20 cm 12.5% polyacrylamide gels casted between low fluorescent glass plates. The strips were overlaid with 0.5% (w/v) low melting point agarose in a running buffer containing bromophenol blue. The gels were run in an Ettan Twelve gel tank (GE Healthcare) at 4.5 W per gel at 10 °C until the dye front had completely run off the bottom of the gels. Afterward, the fluorescence 2-DE was scanned directly between the low fluorescent glass plates using an Ettan DIGE Imager (GE Healthcare). This imager is a charge-coupled device-based instrument that enables scanning at different wavelengths for Cy2-, Cy3-, and Cy5-labeled samples. Gel analysis was performed using DeCyder 2-D Differential Analysis Software v7.0 (GE Healthcare) to co-detect, normalize and quantify the protein features in the images. Features detected from non-protein sources (e.g. dust particles and dirty backgrounds) were filtered out. Spots displaying a $\geqq$1.3 average-fold increase or decrease in abundance with a p-value < 0.05 were selected for protein identification.

2.6. Protein staining, in-gel digestion and MALDI-TOF MS analysis

Colloidal coomassie blue G-250 staining was used to visualize CyDye-labeled protein features in 2-DE followed by excised interested post-stained gel pieces for MALDI-TOF MS identification. The detailed procedures for protein staining, in-gel digestion, MALDI-TOF MS analysis and the algorithm used for data processing were described in our previous publication (Lai et al., 2010). The spectrometer was also calibrated with a peptide calibration standard (Bruker Daltonics) and internal calibration was performed using trypsin autolysis peaks at m/z 842.51 and m/z 2211.10. Peaks in the mass range of m/z 800–3000 were used to generate a peptide mass fingerprint that was searched against the Swiss-Prot/TrEMBL database (v57.12) with 513,877 entries using Mascot software v2.2.06 (Matrix Science, London, UK). The following parameters were used for the search: *Rodent*; tryptic digest with a maximum of 1 missed cleavage; carbamidomethylation of cysteine, partial protein N-terminal acetylation, partial methionine oxidation and partial modification of glutamine to pyroglutamate and a mass tolerance of 50 ppm. Identification was accepted based on significant MASCOT Mowse scores (p < 0.05), spectrum annotation and observed versus expected molecular weight and p*I* on 2-DE.

2.7. Immunoblotting analysis

Immunoblotting analysis was used to validate the differential abundance of mass spectrometry identified proteins. The detailed experimental procedures were described in our previous reports (Hung et al., 2011; Lin et al., 2011; Chen et al., 2011b). All of primary antibodies used for expression validation were purchased from Genetex (Hsinchu, Taiwan).

3. Results

3.1. HA facilitates cell viability in ischemia–reperfusion-induced cell death in H9C2 cells

To evaluate the effect of ischemia–reperfusion on rat cardiomyocytes (H9C2), we exposed these cells to H_2O_2 in a range of 0–1000 μM for 24 h in serum free medium. A MTT assays was performed to determine the H_2O_2-induced cell death. After exposure to H_2O_2, dose dependent loss of cell viabilities has been observed in H9C2 with H_2O_2 concentrations between 300 μM and 600 μM in three independent experiments (Fig. 1). At the concentration of 400 μM, a significant loss (50%) of cell viability was detected at 24 h. In order to verify the role of HA on repair of H_2O_2-induced damage in H9C2 cells, we investigated the changes of cell viability in H9C2 cells incubated in indicated concentrations of LMW-HA or HMW-HA for 30 min followed by exposing to 400 μM H_2O_2 for 24 h. Our data demonstrated that the cell viability was significantly improved by use of HMW-HA; on the other hand, there was no statistically significant difference in cell viability after the addition of 0.05%/0.3% LMW-HA or 0.05% HMW-HA (Fig. 2). The result confirmed HMW-HA but not LMW-HA has the ability to block H9C2 cell death induced by H_2O_2.

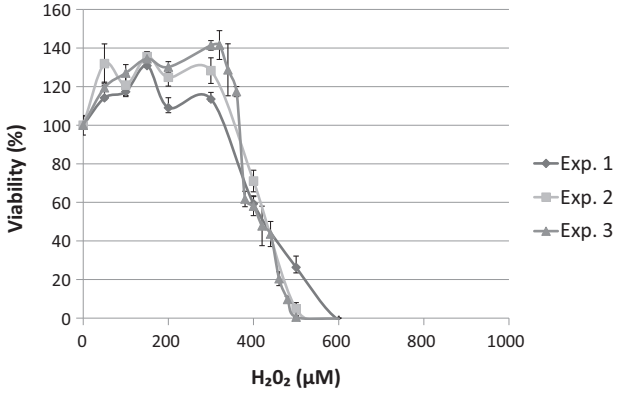

Fig. 1. Effect of H_2O_2 treatment on H9C2 cell viability. H9C2 cells were treated with indicated concentrations of H_2O_2 for three independent experiments. Cell viability was determined by MTT cell viability assay 24 h after H_2O_2 treatment. Each data point indicates mean ± SD of triplicate values.

3.2. HMW-HA facilitates wound healing in H_2O_2-damaged H9C2 cells

In order to study the effect of HA on wound healing of cardiomyocytes, various doses of LMW-HA and HMW-HA on wound closure in H9C2 were examined. Fig. 3 shows the chronological changes in the areas of 400 μM H_2O_2-induced H9C2 cell defects followed by incubating in serum free medium containing 0%, 0.05% or 0.3% LMW-HA or HMW-HA. The results indicated that cardiomyocyte wound healing was rather slow within 8 h after wounding and then became accelerated through 8–24 h. Interestingly, a positive healing influence was observed in H_2O_2-damaged H9C2 cells after the treatment of 0.3% HMW-HA (Fig. 3A). Compared to this condition, the restore of wounded areas was found to reduce significantly when H9C2 cells were incubated in 0.05% LMW-HA, 0.05% HMW-HA or left untreated (Fig. 3B). These results implied 0.3% HMW-HA has profound effect on H_2O_2-induced cardiomyocyte wound healing.

3.3. Global analysis of protein expression in untreated or H_2O_2-treated H9C2 cells with or without HMW-HA treatment

In order to better understand the rat cardiomyocytes response to H_2O_2-induced signalings of cell death and HMW-HA-mediated

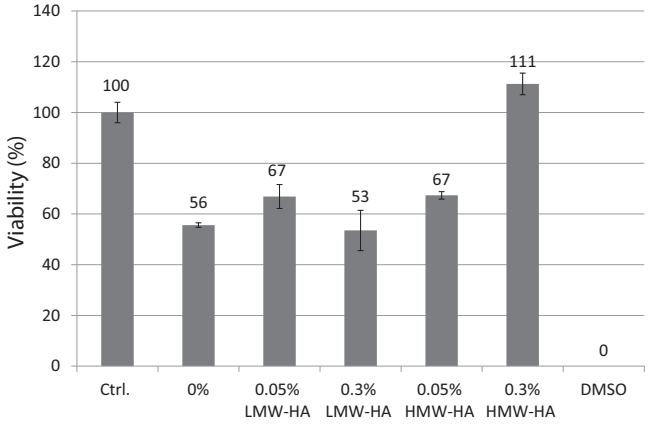

Fig. 2. Effect of low- and high-molecular weight hyaluronic acid on H9C2 cell viability after H_2O_2 treatment. H9C2 cells were pre-incubated with 0.05% or 0.3% low- and high-molecular weight hyaluronic acid for 30 min followed by treated with 400 μM H_2O_2 in serum free medium for 24 h. After removal of H_2O_2, cell viability was subsequently determined by MTT cell viability assay. DMSO treatment groups were served as a negative control. Data are mean ± SD of six independent experiments.

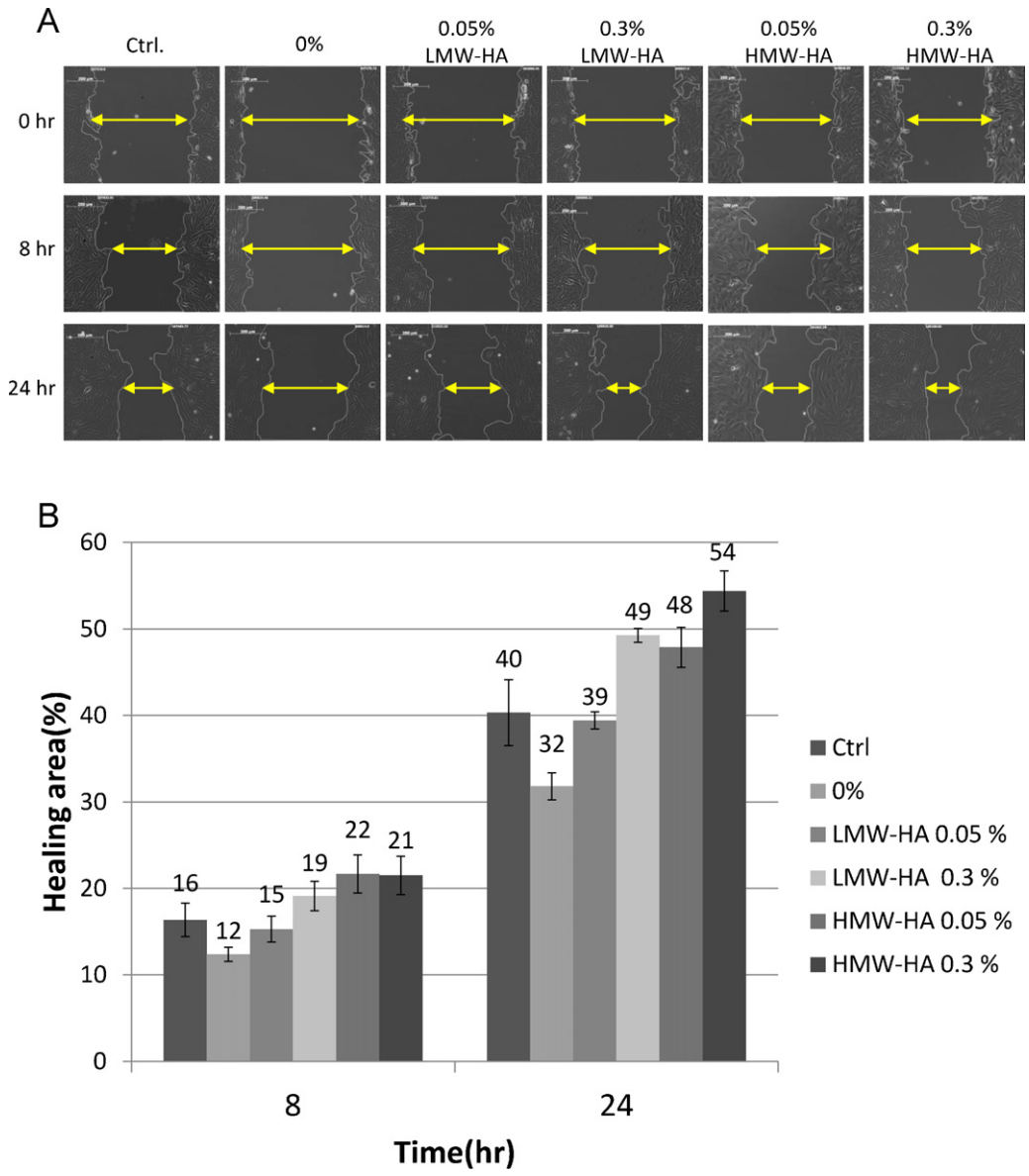

Fig. 3. Effect of hyaluronic acid on H_2O_2 treated cardiomyocyte wound closure in H9C2 cells. The wound cardiomyocytes (H9C2) were treated with indicated concentrations of low- or high-molecular weight hyaluronic acid in serum free medium or with serum free medium alone for 30 min followed by treated with 400 μM H_2O_2 in serum free medium for 24 h. After removal of H_2O_2, the wound healing of H9C2 cells was photographed at the indicated times (A). Each treatment condition has been performed at least 3 times. The relative wound healing rates between 8 h/0 h and 24 h/0 h are shown in (B).

protection pathways, a 2D-DIGE experiment was performed to examine the protein expression changes in untreated H9C2 cells or pre-treated with H_2O_2 followed by treated with 0.05% or 0.3% HMW-HA. The analysis revealed more than 222 protein features displayed differential expression (>1.3-fold; $p < 0.05$) between the 4 different conditions were identified by 2D-DIGE analysis (Fig. 4). Proteins in 167 of these features were subsequently identified by MALDI-TOF MS (Table 1). These differentially expressed proteins mostly have functions in cytoskeleton regulation, protein biosynthesis and protein folding. Interestingly, these differentially expressed proteins are associated with a result of decreased folding-related proteins (such as 78 kDa glucose-regulated protein), ATP synthesis protein (such as ATP synthase), biosynthesis-regulated proteins (such as nucleoside diphosphate kinase A), catabolism-regulated proteins (such as alpha-enolase), growth-related proteins (such as alpha-enolase galectin-1), cytoskeleton regulatory proteins (such as fascin), nuclear assembly-associated proteins (such as prelamin-A/C) and vesicle trafficking protein (such as optineurin) in our proteomic analysis (Fig. 5 and Table 1). Notably, 93 out of the 167 identified proteins showed H_2O_2-dependent changes that were at least partially reversed by HA-treatment (including Fascin and ezrin). For example, protein spot 678 (Fascin), was 1.67-fold down-regulated by H_2O_2-treatment, but recovered to become 1.11-fold and 1.01-fold down-regulated when these cells were treated with 0.05% or 0.3% HMW-HA, respectively (Fig. 6). In addition, protein spot 219, identified as ezrin, was −1.35-fold down-regulated by H_2O_2-treatment, but significantly recovered when pre-treated with 0.3% HMW-HA (Table 1). These data confirm that HMW-HA can partially, if not completely, rescue H_2O_2-induced signals of cell death which are essential for cardiomyocyte repairing processes such as cell survival, cell migration and wound healing.

3.4. HMW-HA-modulated survival- and cytoskeletal-proteins in heart ischemia–reperfusion model

It is interesting and important to know how the HMW-HA modulates cell survival and promotes wound healing during

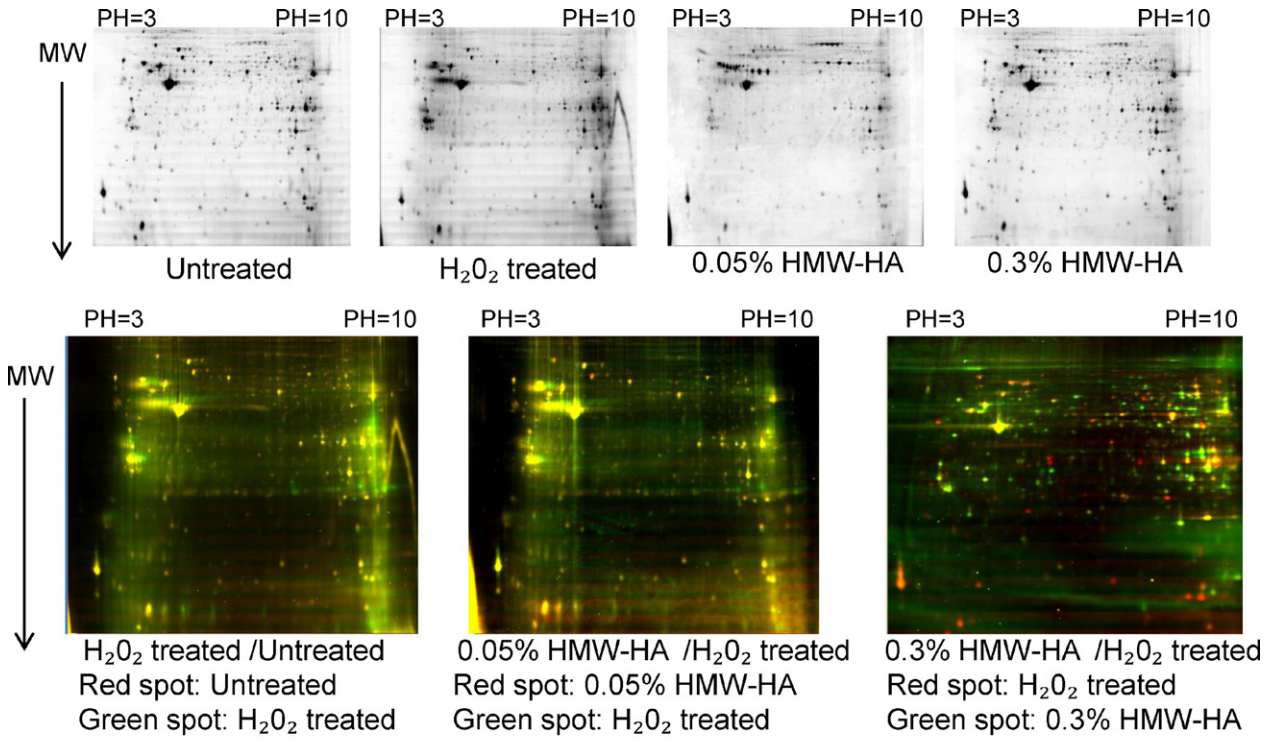

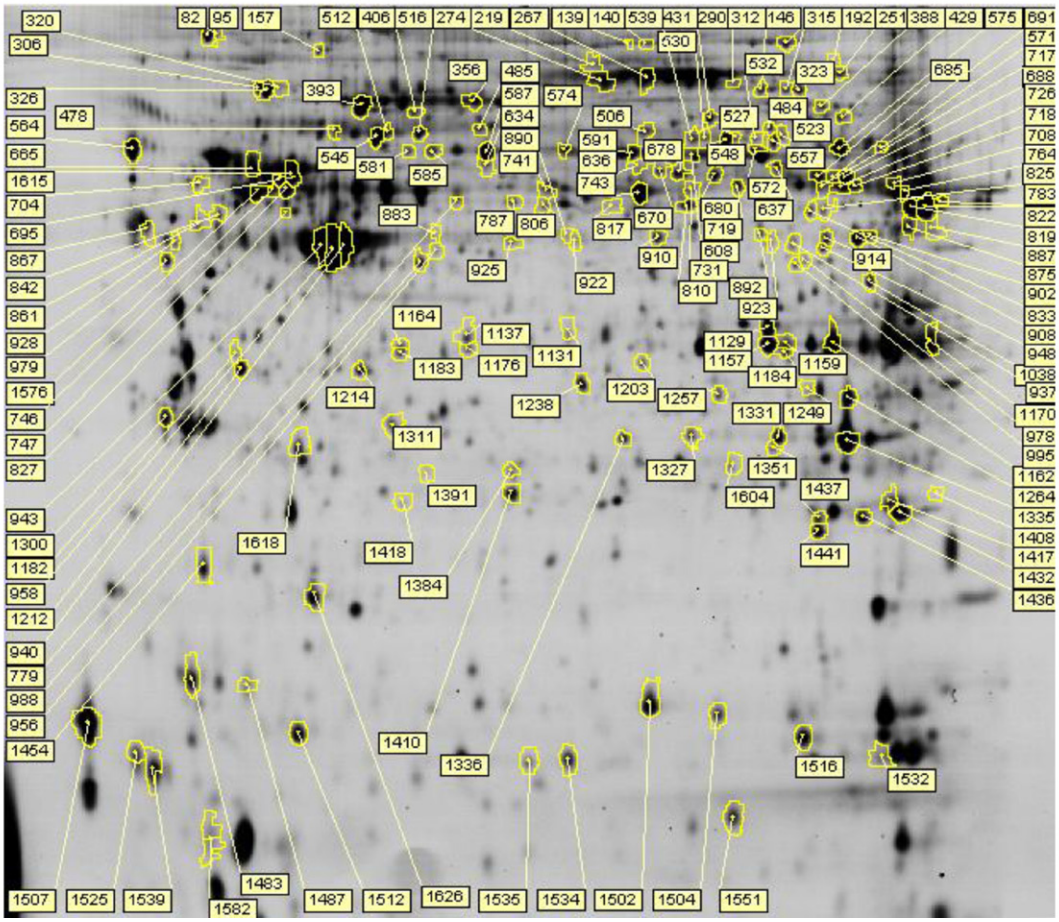

Fig. 4. 2D-DIGE analysis of H_2O_2-induced differential protein expression profiles in rat cardiomyocyte with pre-treated by high molecular weight hyaluronic acid or left untreated. Total cellular proteins (100 μg each) purified from PBS buffer containing 400 μM H_2O_2 or PBS buffer alone treated H9C2 cells after treated with indicated concentrations of high molecular weight hyaluronic acid for 24 h were labeled with Cy-dyes and separated using 24 cm, pH 3–10 non-linear IPG strips followed by resolved with 12.5% SDS-PAGE. 2D-DIGE images of untreated H9C2 cells and H_2O_2-treated H9C2 cells followed by incubated with various concentrations of HMW-HA at appropriate excitation and emission wavelengths were pseudo-colored and overlaid with ImageQuant Tool (GE Healthcare) (upper and middle panels). The MALDI-TOF MS identified differentially expressed protein features are annotated with spot numbers (bottom panels).

Table 1
Alphabetical list of identified differentially expressed proteins across various concentrations of hyaluronic acid-induced protective effects against ischemia–reperfusion in rat cardiomyocytes obtained after 2D-DIGE coupled with MALDI-TOF MS analysis. Average ratios of differential expression ($p < 0.05$) across H9C2 cell, H9C2 cell treated with/without high molecular weight hyaluronic acid followed by incubated with 400 μM H_2O_2 were calculated from triplicate gels. Gray shaded cells indicate protein changes are shown as ≧1.3-fold alternations in relative protein abundance.

Spot No.	Gene name	Swiss-prot No.	Protein name	MW	pI	No. matched / supplied peptides	score	cov. (%)	H_2O_2-treated / Untreated	0.05%HA / Untreated	0.3%HA / Untreated	0.05%HA / H_2O_2 treated	0.3%HA / H_2O_2 treated	Functional classification	subcellular location	matched peptides
827	Psmc4	Q63570	26S protease regulatory subunit 6B	47493	5.09	7/14	92/51	14%	1.94	-1.09	-1.49	-2.11	-2.89	Proteolysis	Cytoplasm	K.AVAHHTTAAFIR.V R.VVGSEFVQK.Y
787	Psmc2	Q63347	26S protease regulatory subunit 7	48943	5.59	15/29	156/51	34%	-1.46	1.05	-1.1	1.53	1.33	Proteolysis	Cytoplasm	R.EVVETPLLHPER.F R.FVNLGIEPPK.G
833	Psmc5	P62198	26S protease regulatory subunit 8	45768	7.11	6/12	88/51	16%	-1.75	-1.53	-1.47	1.14	1.19	Proteolysis	Cytoplasm	R.IDILDSALLRPGR.I K.IEFPPPNEEAR
523	Mrps7	Q5I0K8	28S ribosomal protein S7, mitochondrial	28350	10.03	7/18	73/51	28%	-1.36	-1.23	-1.3	1.1	1.04	Protien synthesis	Mitochondrion	K.QVSELTEEEK.Y R.SLMAQTLEAVK.R
1551	Rps12	P63324	40S ribosomal protein S12	14858	6.82	6/27	94/51	48%	-1.76	-1.36	-1.28	1.3	1.37	Protien synthesis	Cytoplasm	K.TALIHDGLAR.G K.LGEWVGLCK.I
545	Hspd1	P63039	60 kDa heat shock protein, mitochondrial	61088	5.91	15/28	158/51	29%	-1.98	-1.95	-2.4	1.02	-1.21	Protein folding	Mitochondrion	K.QSKPVTTPEEIAQVATISANGDK.D K.DGKTLNDELEIIEGMK.F
1311	Pgls	P85971	6-phosphogluconolactonase	27445	5.54	6/37	85/57	31%	-1.64	-1.28	-1.23	1.28	1.33	Catabolism	Cytoplasm	R.VAPEEHPVLLTEAPLNPK.A R.DLTDYLMK.I
306	Hspa5	P06761	78 kDa glucose-regulated protein	72473	5.07	9/16	114/57	12%	-1.86	-1.23	1.48	1.51	2.75	Protein folding	ER	R.LTPEEIER.M KITITNDQNR.L
320	Hspa5	P06761	78 kDa glucose-regulated protein	72473	5.07	19/44	161/51	32%	-1.65	-1.18	-1.43	1.4	1.15	Protein folding	ER	K.VYEGERPLTK.D K.DNHLLGTFDLTGIPPAPR.G
323	Hspa5	P06761	78 kDa glucose-regulated protein	72473	5.07	19/47	155/57	32%	-1.81	1.04	1.36	1.88	2.47	Protein folding	ER	K.ITITNDQNR.L R.LTPEEIER.M
326	Hspa5	P06761	78 kDa glucose-regulated protein	72473	5.07	11/23	132/57	16%	-1.93	-1.62	-1.66	1.2	1.17	Protein folding	ER	K.DNHLLGTFDLTGIPPAPR.G K.ITITNDQNR.L
995	Acat2	Q5XI22	Acetyl-CoA acetyltransferase, cytosolic	41538	6.86	6/22	58/51	14%	-1.99	-1.36	-2.01	1.46	-1.01	Catabolism	Cytoplasm	K.ELGLSPEK.V R.ILVTLLHTLERVGGTR.G
251	Aco2	Q9ER34	Aconitate hydratase, mitochondrial	86121	7.87	6/15	72/51	7%	-1.68	-1.48	-2.32	1.13	-1.38	Catabolism	Mitochondrion	K.FNPETDFLTGK.D R.NAVTQEFGPVPDTAR.Y
958	Acta2	P68035	Actin, alpha cardiac muscle 1	42334	5.23	14/53	90/51	30%	-1.57	-1.25	-1.05	1.25	1.49	Cytoskeleton	Cytoplasm	R.AVFPSIVGRPR.H R.HQGVMVGMGQK.D
883	Actb	P60711	Actin, cytoplasmic 1	42052	5.29	8/16	108/51	23%	-1.6	-1.11	-1.4	1.44	1.15	Cytoskeleton	Cytoplasm	R.GYSFTTTAER.E K.SYELPDGQVITIGNER.F
890	Actb	P60711	Actin, cytoplasmic 1	42052	5.29	8/28	92/51	25%	-1.24	1.28	1.38	1.58	1.71	Cytoskeleton	Cytoplasm	K.SYELPDGQVITIGNER.F K.DLYANTVLSGGTTMYPGIADR.M
925	Actb	P60711	Actin, cytoplasmic 1	42052	5.29	7/21	91/51	17%	-1.76	-1.74	-1.92	1.01	-1.1	Cytoskeleton	Cytoplasm	R.GYSFTTTAER.E K.SYELPDGQVITIGNER.F
940	Actb	P60711	Actin, cytoplasmic 1	42052	5.29	19/54	165/51	51%	-1.54	-1.35	-1.04	1.14	1.49	Cytoskeleton	Cytoplasm	K.DSYVGDEAQSKR.G K.IWHHTFYNELR.V
958	Actb	P60711	Actin, cytoplasmic 1	42052	5.29	19/53	144/51	44%	-1.57	-1.25	-1.05	1.25	1.49	Cytoskeleton	Cytoplasm	K.IWHHTFYNELR.V R.VAPEEHPVLLTEAPLNPK.A

Table 1 (*Continued*)

1331	Actb	P60711	Actin, cytoplasmic 1	42052	5.29	9/21	108/51	30%	-1.57	-1.37	-1.26	1.14	1.25	Cytoskeleton	Cytoplasm	R.GYSFTTTAER.E K.SYELPDGQVITIGNER.F
943	Actg2	P63269	Actin, gamma-enteric smooth muscle	42249	5.31	11/57	80/57	27%	-1.57	-1.3	-1.12	1.21	1.41	Cytoskeleton	Cytoplasm	K.RGILTLK.Y R.VAPEEHPTLLTEAPLNPK.A
806	Abra	Q8K4K7	Actin-binding Rho-activating protein	43046	7.28	6/15	61/51	19%	-1.68	-1.24	-1.16	1.36	1.45	Cytoskeleton	Cytoplasm	R.YSETLNCKAHR.K K.YSQVDNLKGR.W
779	Actr3b	Q4V7C7	Actin-related protein 3	47783	5.61	13/42	111/51	28%	-1.79	1.01	1.12	1.82	2	Cytoskeleton	Cytoplasm	R.DITYFIQQLLR.D R.DREVGIPPEQSLETAK.A
923	Lrpap1	Q99068	Alpha-2-macroglobulin receptor-associated protein	42006	6.85	7/18	60/51	16%	-1.37	1.03	-1.08	1.41	1.27	Lipase binding	Plasma membrane	R.SINQGLDR.L K.HVESIGDPEHISR.N
937	Lrpap1	Q99068	Alpha-2-macroglobulin receptor-associated protein	42006	6.85	8/22	76/57	23%	-1.56	-1.32	-1.39	1.19	1.13	Lipase binding	Plasma membrane	K.VSHQGYGPATEFEEPR.V K.ELESFREELK.H
743	Eno1	P04764	Alpha-enolase	47440	6.16	10/19	111/51	18%	-1.75	-1.44	-1.4	1.21	1.25	Catabolism	Cytoplasm	K.KLNVVEQEK.I R.IGAEVYHNLK.N
1157	Anxa1	P07150	Annexin A1	39147	6.97	28/72	218/57	74%	-1.62	-1.4	-1.34	1.16	1.2	Exocytosis	Plasma membrane	R.SAPAATVCPEHCDPTR.C R.CAPPPTDCEGGR.V
1159	Anxa1	P07150	Annexin A1	39147	6.97	7/35	78/57	21%	-1.64	-1.13	1.02	1.45	1.67	Exocytosis	Plasma membrane	K.GLGTDEDTLIEILTTR.S K.DITSDTSGDFR.N
1129	Anxa1	P07150	Annexin A1	39147	6.97	6/15	63/51	15%	-1.57	-1.56	-1.42	1.01	1.1	Exocytosis	Plasma membrane	R.ALYEAGER.R K.GTDVNVFNTILTTR
1162	Anxa2	Q07936	Annexin A2	38939	7.55	18/56	136/57	43%	-1.63	-1.26	1.01	1.3	1.65	Anti-coagulation	Secreted	R.VLSIGDGIAR.V R.TGAIVDVPVGDELLGR.V
1238	Anxa3	P14669	Annexin A3	36569	5.96	19/69	142/57	46%	-1.97	-1.55	-1.55	1.27	1.27	Anti-coagulation	Plasma membrane	R.FHVEEEGKGK.D K.LGDVYVNDAFGTAHR.A
1214	Anxa4	P55260	Annexin A4	36168	5.31	10/50	109/57	31%	-1.46	-1.21	-1.07	89/	1.37	Exocytosis	Plasma membrane	K.TWMGKMQK.K K.GVVEVTHDLQK.H
1212	Anxa5	P14668	Annexin A5	35779	4.93	12/39	122/57	37%	-1.73	-1.36	-1.2	1.27	1.44	Anti-coagulation	Plasma membrane	K.FITILGTR.S K.YMTISGFQIEETIDR.E
948	Got1	P13221	Aspartate aminotransferase, cytoplasmic	46628	6.73	7/22	68/57	11%	-1.3	-1.33	-1.11	-1.02	1.17	Metabolism	Cytoplasm	R.KVNLGVGAYR.T K.VNLGVGAYR.T
717	Atp5a1	P15999	ATP synthase subunit alpha, mitochondrial	59831	9.22	12/37	125/51	19%	-1.07	-1.35	1.55	-1.27	1.65	ATP synthesis	Mitochondrion	R.TGAIVDVPVGDELLGR.V K.APGIIPR.I
718	Atp5a1	P15999	ATP synthase subunit alpha, mitochondrial	59831	9.22	11/22	110/57	19%	-1.47	-1.51	-1.35	-1.03	1.09	ATP synthesis	Mitochondrion	R.TGAIVDVPVGDELLGR.V K.AVDSLVPIGR.G
726	Atp5a1	P15999	ATP synthase subunit alpha, mitochondrial	59831	9.22	9/23	112/57	15%	-1.51	-1.4	-1.09	1.08	1.38	ATP synthesis	Mitochondrion	R.LYGPSSVSFADDFVR.S R.SALQSINEWASQTTDGK.L
1576	Atp5b	P10719	ATP synthase subunit beta, mitochondrial	56318	5.19	14/59	141/51	29%	-2.02	-1.71	-1.59	1.18	1.27	ATP synthesis	Mitochondrion	K.AHGGYSVFAGVGER.T R.VALTGLTVAEYFR.D
1437	Supv3l1	Q5EBA1	ATP-dependent RNA helicase SUPV3L1, mitochondrial	87620	8.18	11/40	76/57	14%	-1.39	-1.19	-1.08	1.17	1.29	RNA metabolism	Mitochondrion	R.RPPNWYPEARAIQR.K R.YLSATSGVYCGPLK.L

1525	Sncb	Q63754	Beta-synuclein	14495	4.48	6/24	84/51	29%	-1.44	-1.31	-1.34	1.1	1.07	Vesicle trafficking	Cytoplasm	K.EGVVAAAEK.T K.QGVTEAAEK.T
484	Atic	O35567	Bifunctional purine biosynthesis protein PURH	64681	6.69	10/26	118/57	15%	-1.69	-1.22	-1.31	1.39	1.29	Biosynthesis	Cytoplasm	R.ICIHTNGR.V K.HYGYTSYSVSDSEK.E
1351	Camk1	Q63450	Calcium/calmodulin-dependent protein kinase type 1	42182	5.19	6/13	58/51	9%	-1.67	-1.52	-1.77	1.1	-1.06	Signal transduction	Cytoplasm	R.WKQAEDIR.D R.HLMEKDPEK.R
1182	Camk1	Q63450	Calcium/calmodulin-dependent protein kinase type 1	42182	5.19	6/24	58/51	13%	-1.69	1.16	-1.39	1.96	1.22	Signal transduction	Cytoplasm	K.QAEDIRDIYDFR.D K.EGSMENEIAVLHK.I
1507	Calm1	P62161	Calmodulin	16827	4.09	7/12	102/51	38%	-1.6	-1.04	1.06	1.53	1.7	Signal transduction	Cytoplasm	K.EAFSLFDKDGDGTITTK.E K.ELGTVMR.S
979	Cnn3	P37397	Calponin-3	36583	5.47	7/38	67/51	22%	-1.49	-1.43	-1.59	1.04	-1.07	Cytoskeleton regulation	Cytoplasm	K.CASQAGMTAYGTRR.H K.GASQAGMSAPGTR.R
564	Calr	P18418	Calreticulin	48137	4.33	17/45	170/57	31%	-1.7	-1.56	-1.39	1.09	1.22	Protein folding	ER	R.GYNDAVSYLR.R K.RVIFPR.V
867	Calu	O35783	Calumenin	37087	4.40	8/30	73/51	23%	-2.8	-2.03	-1.83	1.38	1.53	Metabolism	ER	R.VHHEPQLSDK.V K.SFGQLTPEESKEK.L
634	Pde4d	P14270	cAMP-specific 3',5'-cyclic phosphodiesterase 4D	91123	5.36	6/40	61/51	9%	-1.36	-1.46	-1.26	-1.08	1.08	Catabolism	Cytoplasm	R.SDSDYDLSPK.S R.SPMCNQPSINK.A
1335	Car3	P14141	Carbonic anhydrase 3	29698	6.89	7/46	73/57	28%	-1.6	-1.35	-1.13	1.18	1.41	Redox regulation	Cytoplasm	R.VVFDDTFDR.S R.GGPLSGPYR.L
1618	Ctsb	P00787	Cathepsin B	38358	5.36	9/20	116/51	27%	-1.31	-1.21	-1.15	1.08	1.14	Proteolysis	Lysosome.	R.EQWSNCPTIAQIR.D R.DQGSCGSCWAFGAVEAMSDR.I
1502	Cfl1	P45592	Cofilin-1	18749	8.22	6/27	58/51	32%	-1.59	-1.01	-1.31	1.58	1.22	Cytoskeleton regulation	Plasma membrane	K.AVLFCLSEDKK.N K.NIILEEGK.E
956	Cops4	Q68FS2	COP9 signalosome complex subunit 4	46546	5.60	13/22	161/51	34%	-1.43	1.04	1.08	1.48	1.54	Proteolysis	Cytoplasm	R.VISFEEQVASIR.Q R.LYLEDDDPVQAEAYINR.A
922	Cpox	Q3B7D0	Coproporphyrinogen-III oxidase, mitochondrial	49817	8.80	6/18	65/57	16%	-1.6	-1.14	1.03	1.4	1.64	Biosynthesis	Mitochondrion	R.GDYAQLR.A R.AEMVPKSSGAR.S
557	Mus81	Q4KM32	Crossover junction endonuclease MUS81	62434	9.42	7/21	62/51	11%	-1.72	-1.34	-1.33	1.28	1.3	DNA repair	Nucleus	R.EHLNSDGHSFLTKEELLQK.C K.EELLQKCAQK.T
1487	Cth	P18757	Cystathionine gamma-lyase	44262	8.20	8/30	62/51	19%	1.15	-1.21	-1.29	-1.39	-1.48	Biosynthesis	Cytoplasm	R.SGNPTRNCLEK.A K.HCLTFARGLAATTTITHLLK.A
532	Lap3	Q68FS4	Cytosol aminopeptidase	56514	6.77	6/15	59/51	10%	-1.62	-1.5	-1.68	1.08	-1.04	Proteolysis	Cytoplasm	K.WAHLDIAGVMTNK.D K.DEIPYLRK.G
608	Phgdh	O08651	D-3-phosphoglycerate dehydrogenase	57256	6.28	8/29	88/51	13%	-1.66	-1.15	-1.05	1.44	1.57	Catabolism	Plasma membrane	K.ILQDGGLQVVEK.Q R.AGTGVDNVDLEAATR.K
1504	Dstn	Q7M0E3	Destrin	18807	8.19	8/22	72/51	31%	-1.62	-1.14	-1.45	1.43	1.12	Cytoskeleton regulation	Cytoplasm	K.AVIFCLSADKK.C K.HFVGMLPEK.D

637	Dld	Q6P6R2	Dihydrolipoyl dehydrogenase, mitochondrial	54574	7.96	7/21	76/51	14%	-1.66	-1.61	-1.77	1.03	-1.06	Redox regulation	Mitochondrion	K.ALTGGIAHLFK.Q K.QNKVVHVNGFGK.I
825	Dnaja1	P63036	DnaJ homolog subfamily A member 1	45581	6.65	7/17	73/51	10%	-1.49	-1.48	-1.28	1.01	1.17	Protein folding	Mitochondrion	R.TIVITSHPGQIVK.H K.CVLNEGMPIYR.R
585	Eml1	Q05BC3	Echinoderm microtubule-associated protein-like 1	90650	6.56	7/24	65/51	9%	-1.3	-1.26	-1.25	1.03	1.04	Cytoskeleton regulation	Cytoplasm	K.EVVVPVTK.S R.GRPVTMYMPK.D
810	Eef1g	Q68FR6	Elongation factor 1-gamma	50371	6.31	8/22	84/51	13%	-1.51	-1.06	-1.02	1.42	1.48	Biosynthesis	Cytoplasm	K.AKDPFAHLPK.S K.STFVLDEFKR.K
146	Eef2	P05197	Elongation factor 2	96192	6.41	9/24	79/51	9%	-2.44	-1.83	-2.12	1.33	1.15	Biosynthesis	Cytoplasm	K.FSVSPVVR.V K.SDPVVSYR.E
139	Eef2	P05197	Elongation factor 2	96192	6.41	11/20	91/51	12%	-3.42	-1.5	-1.09	2.29	3.14	Protien synthesis	Cytoplasm	K.DSVVAGFQWATK.E R.GGGQIIPTAR.R
140	Eef2	P05197	Elongation factor 2	96192	6.41	13/33	127/57	15%	-1.75	1	-1.17	1.75	1.5	Protien synthesis	Cytoplasm	R.NMSVIAHVDHGK.S K.QFAEMYVAK.F
1336	Erp29	P52555	Endoplasmic reticulum protein ERp29	28614	6.23	6/13	100/57	24%	-1.72	-1.34	-1.42	1.28	1.21	Protein folding	ER	K.ESYPVFYLFR.D R.DGDFENPVPYSGAVK.V
82	Tra1	Q66HD0	Endoplasmin	92998	4.72	7/15	83/57	9%	-2.04	-1.61	-1.36	1.27	1.5	Protein folding	ER	R.GLFDEYGSK.K K.GVVDSDDLPLNVSR.E
95	Tra1	Q66HD0	Endoplasmin	92998	4.72	23/41	163/57	23%	-1.75	-1.43	-1.34	1.22	1.31	Protein folding	ER	K.YNDTFWK.E K.EFGTNIK.L
1408	Peci	Q5XIC0	Enoyl-CoA delta isomerase 2, mitochondrial	43336	9.11	7/29	63/51	19%	2.73	1.26	-1.13	-2.16	-3.09	Metabolism	Peroxisome	K.WDAWNALGSLPK.E K.ITFNRPSKK.N
219	Ezr	P31977	Ezrin	69462	5.83	6/21	69/51	8%	-1.35	-1.15	1.01	1.18	1.36	Cytoskeleton regulation	Plasma membrane	K.IGFPWSEIR.N K.APDFVFYAPR.L
388	Trx2	Q32PX7	Far upstream element-binding protein 1	67326	7.18	10/16	111/57	16%	-1.14	1.47	-1.3	1.68	-1.14	Gene regulation	Nucleus	K.KIQNDAGVR.I R.IQFKPDDGTTPDR.I
678	Fscn1	P85845	Fascin	55215	6.44	7/16	103/51	15%	-1.67	-1.11	-1.01	1.49	1.65	Cytoskeleton regulation	Cytoplasm	R.LVARPEPATGFTLEFR.S K.NASCYFDIEWCER.R
680	Fscn1	P85845	Fascin	55215	6.44	12/36	107/51	22%	-1.94	-1.42	-1.34	1.37	1.45	Cytoskeleton regulation	Cytoplasm	R.YLAPSGPSGTLKAGK.A K.LINRPIIVFR.G
356	Fgg	P02680	Fibrinogen gamma chain	51228	5.62	6/21	60/51	14%	4.54	1.85	4.29	-2.46	-1.06	Coagulation	Secreted	R.IQLKDWSGR.T K.FFTSHNGMHFSTWDNDNDK.F
1582	Lgals	P11762	Galectin-1	15189	5.14	6/35	80/57	47%	1.53	2.41	-1.06	1.57	-1.63	Cell growth	Secreted	K.GENLSLVVHGPGDIR.L R.IGDFVVK.K
708	Gsn	Q68FP1	Gelsolin	86413	5.76	9/32	72/51	8%	-1.02	-1.99	-1.44	-1.96	-1.41	Cytoskeleton regulation	Cytoplasm	R.EVQGFESSTFQGYFK.S R.DGGQTTPASTR.L
988	Glrx3	Q9JLZ1	Glutaredoxin-3	38111	5.51	8/21	96/57	27%	-1.68	-1.29	-1.21	1.31	1.39	Redox regulation	Cytoplasm	K.EHPHVSFVK.L R.HVSSGSFPPSTNEHVK.E
1441	Ran	P62828	GTP-binding nuclear protein Ran	24579	7.01	6/25	91/57	24%	-1.87	-1.37	-1.05	1.37	1.79	Transport	Nucleus	K.FNVWDTAGQEK.F K.NVPNWHR.D

1164	Gnb1	P54311	Guanine nucleotide-binding protein G(I)/G(S)/G(T) subunit beta-1	38151	5.60	7/11	99/51	20%	-1.8	-1.02	-1.14	1.76	1.57	Signal transduction	Plasma membrane	R.EGNVRVSR.E R.ELAGHTGYLSCCR.F
1183	Gnb2	P54313	Guanine nucleotide-binding protein G(I)/G(S)/G(T) subunit beta-2	38048	5.60	8/25	108/51	20%	-1.67	-1.03	1.06	1.62	1.76	Signal transduction	Plasma membrane	R.ELPGHTGYLSCCR.F R.TFVSGACDASIK.L
1264	Gnb2l1	P63245	Guanine nucleotide-binding protein subunit beta-2-like 1	35511	7.60	7/14	94/57	27%	-1.6	-1.17	-1.01	1.36	1.58	Signal transduction	Plasma membrane	K.DVLSVAFSSDNR.Q K.LWNTLGVCK.Y
393	Hspa8	P63018	Heat shock cognate 71 kDa protein	71055	5.37	10/27	84/51	21%	-1.75	-1.5	-1.33	1.16	1.32	Protein folding	Cytoplasm	K.DAGTIAGLNVLR.I K.STAGDTHLGGEDFDNR.M
1410	Hspb1	P42930	Heat shock protein beta-1	22936	6.12	6/38	72/57	20%	-1.32	-1.29	-1.5	1.02	-1.14	Protein folding	Cytoplasm	R.SPSWEPFR.D R.DWYPAHSR.L
192	Hsp90aa1	P82995	Heat shock protein HSP 90-alpha	85161	4.93	7/17	69/51	9%	-1.51	1.2	1.08	1.81	1.63	Protein folding	Cytoplasm	K.SLTNDWEEHLAVK.H K.HFSVEGQLEFR.A
741	Hnrnph1	Q8VHV7	Heterogeneous nuclear ribonucleoprotein H	49442	5.70	8/18	105/51	16%	-1.71	-1.34	-1.25	1.27	1.36	Gene regulation	Nucleus	K.HTGPNSPDTANDGFVR.L R.YIEIFK.S
512	Hnrnpk	P61980	Heterogeneous nuclear ribonucleoprotein K	51230	5.39	9/33	70/51	21%	-1.76	-1.41	-1.69	1.25	1.04	Gene regulation	Nucleus	R.TDYNASVSVPDSSGPER.I K.GSDFDCELR.L
1170	Hnrnpa2b1	A7VJC2	Heterogeneous nuclear ribonucleoproteins A2/B1	37512	8.97	6/13	97/51	18%	-1.8	-1.45	-1.63	1.24	1.1	Gene regulation	Nucleus	K.LTDCVVMR.D R.EESGKPGAHVTVK.K
928	Ido1	Q9ERD9	Indoleamine 2,3-dioxygenase 1	75973	7.83	7/19	67/57	10%	-1.57	-1.14	-1.3	1.38	1.21	Biosynthesis	Cytoplasm	K.ALCSIAASLEKAK.E K.FSGGSAGQSSIFQSLDVLLGIK.H
539	Ica1l	Q6RUG5	Islet cell autoantigen 1-like protein	49298	5.23	8/39	69/57	28%	-1.41	-1.11	-1.17	1.26	1.21	Signal transduction	Cytoplasm	K.VALSEEEERFER.E K.QEVATFSQR.A
892	Idh1	P41562	Isocitrate dehydrogenase [NADP] cytoplasmic	47047	6.53	9/19	85/51	17%	-1.42	-1.2	-1.33	1.19	1.07	Metabolism	Mitochondrion	R.HAYGDQYR.A R.ATDFVVPGPGK.V
875	Idh2	P56574	Isocitrate dehydrogenase [NADP], mitochondrial	51391	8.88	8/11	125/51	15%	-1.55	-1.48	-1.68	1.05	-1.08	Metabolism	Mitochondrion	R.NILGGTVFR.E R.HAHGDQYK.A
817	Krt10	Q6IFW6	Keratin, type I cytoskeletal 10	56699	5.10	14/65	75/51	22%	-1.3	1.3	1.09	1.68	1.41	Cytoskeleton	Cytoplasm	K.SSLGGGYSSGGFSGGSFSR.G K.VTMQNLNDR.L
1176	Ldhb	P42123	L-lactate dehydrogenase B chain	36874	5.70	11/33	123/57	32%	-1.59	-1.15	1.03	1.38	1.65	Catabolism	Cytoplasm	K.IVVVTAGVR.Q R.LNLVQR.N
685	Slc25a11	P97700	Mitochondrial 2-oxoglutarate/malate carrier protein	34393	9.89	8/32	66/51	19%	-1.57	-1.55	-1.33	1.02	1.18	Transport	Mitochondrion	R.MTADGRLPADQR.R R.LPADQRR.G
506	Mfn1	Q8R4Z9	Mitofusin-1	84649	6.11	11/46	69/51	15%	-1.56	-1.42	-1.5	1.1	1.04	Mitochondrial fusion	Mitochondrion	R.WDASASEPEYMEDVRR.Q K.VVSPLEAR.N
1539	Myl6	Q64119	Myosin light polypeptide 6	17135	4.46	6/15	95/51	35%	-1.62	-1.49	-1.22	1.09	1.33	Cytoskeleton	Cytoplasm	R.ALGQNPTNAEVLK.V K.DQGTYEDYVEGLR.V
1483	Myl12b	P18666	Myosin regulatory light chain 12B	19883	4.78	7/29	82/51	36%	-1.54	-1.33	-1.17	1.16	1.31	Cytoskeleton	Cytoplasm	K.EAFNMIDQNR.D K.EDLHDMLASLGK.N

485	RGD1309537	P13832	Myosin regulatory light chain RLC-A	19940	4.67	12/36	96/57	43%	-1.46	-1.07	-1.49	1.37	-1.02	Cytoskeleton	Cytoplasm	K.DLPESALR.D K.DGQVIGIGAGQQSR.I
267	Renbp	P51607	N-acylglucosamine 2-epimerase	50143	5.48	7/19	67/57	10%	-1.62	-1.16	1.16	1.4	1.88	Metabolism	Cytoplasm	R.ETLQVWK.Q R.DGQVYDHLK.Y
1604	Nrxn1	Q63372	Neurexin-1-alpha	170211	5.65	7/16	60/51	4%	-1.41	1.16	-1.06	1.64	1.33	Cell adhesion	Plasma membrane	R.LAIARQR.I K.GRQLTIFNSQATIIIGGK.E
1512	Nme1	Q05982	Nucleoside diphosphate kinase A	17296	5.96	8/20	112/57	48%	-1.82	-1.43	-1.28	1.27	1.42	Biosynthesis	Cytoplasm	R.DDISSETSGDFRK.A K.ALLTLADGGR.D
1535	Nme1	Q05982	Nucleoside diphosphate kinase A	17296	5.96	6/30	82/57	34%	-1.67	-1.24	-1.44	1.34	1.16	Biosynthesis	Cytoplasm	R.TFIAIKPDGVQR.G R.GLVGEIIK.R
1516	Nme2	P19804	Nucleoside diphosphate kinase B	17386	6.92	7/37	103/51	41%	-1.59	-1.3	-1.21	1.22	1.32	Biosynthesis	Cytoplasm	K.DRPFFPGLVK.Y R.VMLGETNPADSKPGTIR.G
1249	Optn	Q8R5M4	Optineurin	67656	5.03	6/28	67/51	10%	-1.53	-1.08	-1.1	1.42	1.39	Vesicle trafficking	Cytoplasm	K.ALSHENER.L R.LATLQATHDK.L
1532	Ppia	P10111	Peptidyl-prolyl cis-trans isomerase A	18091	8.34	8/34	83/51	26%	1.17	-1.21	-1.37	-1.41	-1.6	Protein folding	Cytoplasm	K.FEDENFILK.H K.VKEGMSIVEAMER.F
581	Fkbp4	Q9QVC8	Peptidyl-prolyl cis-trans isomerase FKBP4	51817	5.46	10/27	79/51	15%	-1.51	-1	-1.37	1.51	1.11	Protein folding	Cytoplasm	K.GEHSIVYLKPSYAFGSVGK.E R.FQIPPHAELR.Y
887	Prph	P21807	Peripherin	53631	5.37	9/28	72/51	15%	-1.86	-1.65	-1.66	1.13	1.12	Cytoskeleton	Cytoplasm	R.LLGSGSPSSSAR.L R.LGSFRAPR.A
1432	Prdx1	Q63716	Peroxiredoxin-1	22323	8.27	10/51	145/57	43%	-1.34	-1.23	-1.3	1.09	1.03	Redox regulation	Cytoplasm	K.AAYLQETGKPLDETLKK.A K.TPAQFDADELR.A
1436	Prdx1	Q63716	Peroxiredoxin-1	22323	8.27	7/29	84/57	31%	2.61	2.86	3.26	1.1	1.25	Redox regulation	Cytoplasm	R.TIAQDYGVLK.A K.ADEGISFR.G
1626	Prdx2	P35704	Peroxiredoxin-2	21941	5.34	8/39	108/51	27%	-1.54	-1.41	-1.29	1.1	1.19	Redox regulation	Cytoplasm	R.QITVNDLPVGR.S R.SVDEALR.L
1384	Prdx6	O35244	Peroxiredoxin-6	24860	5.64	6/17	87/57	26%	-1.84	-1.37	-1.78	1.34	1.03	Redox regulation	Cytoplasm	K.LPFPIIDDKDR.D R.VVFIFGPDK.K
1391	Prdx6	O35244	Peroxiredoxin-6	24860	5.64	7/15	102/57	24%	-1.03	1.57	1.24	1.62	1.27	Redox regulation	Cytoplasm	K.DSNNLCLHFNPR.F K.DDGTWGTEQR.E
1203	Pitpna	P16446	Phosphatidylinositol transfer protein alpha isoform	32115	5.97	9/37	86/51	22%	-1.39	-1.04	1.08	1.34	1.49	Transport	Cytoplasm	R.QLFCWLDK.W K.WVDLTMDDIR.R
902	Pgk1	P16617	Phosphoglycerate kinase 1	44909	8.02	9/26	78/51	19%	-1.42	-1.41	-1.35	1.01	1.05	Catabolism	Cytoplasm	R.FHVEEEGKGK.D K.LGDVYVNDAFGTAHR.A
908	Pgk1	P16617	Phosphoglycerate kinase 1	44909	8.02	6/13	65/51	16%	-1.63	-1.4	-1.27	1.16	1.28	Catabolism	Cytoplasm	K.LGDVYVNDAFGTAHR.A R.AHSSMVGVNLPQK.A
1327	Pgam1	P25113	Phosphoglycerate mutase 1	28928	6.67	6/26	105/51	35%	-1.8	-1.03	-1.27	1.75	1.42	Catabolism	Cytoplasm	R.HGESAWNLENR.F R.FSGWYDADLSPAGHEEAK.R
406	Pls3	Q63598	Plastin-3	71148	5.32	11/28	133/51	18%	-1.01	-1.11	1.35	-1.09	1.37	Cytoskeleton regulation	Cytoplasm	K.INNFSADIK.D R.QFVTPADVVSGNPK.L
691	Hmbs	P19356	Porphobilinogen deaminase	39622	6.21	6/15	58/51	10%	-1.7	-1.35	-1.13	1.26	1.51	Biosynthesis	Cytoplasm	R.VAQLQRK.F R.KFPHLEFK.S
290	Lmna	P48679	Prelamin-A/C	74564	6.54	11/19	141/51	16%	-1.28	1.41	1.43	1.81	1.83	Nuclear assembly	Nucleus	K.EGDLLAAQAR.L R.TLEGELHDLR.G

312	Lmna	P48679	Prelamin-A/C	74564	6.54	15/32	137/51	22%	-1.45	-1.25	-1.21	1.16	1.2	Nuclear assembly	Nucleus	R.NSNLVGAAHEELQQSR.I R.EMAEMRAR.M
315	Lmna	P48679	Prelamin-A/C	74564	6.54	6/13	82/51	10%	-1.65	-1.14	-1.01	1.44	1.63	Nuclear assembly	Nucleus	R.SGAQASSTPLSPTR.I R.SLETENAGLR.L
1137	Phb	P67779	Prohibitin	29859	5.57	6/28	86/51	23%	-1.74	-1.1	-1.04	1.58	1.68	Cell growth	Mitochondrion	K.DLQNVNITLR.I R.IYTSIGEDYDER.V
1417	Psmb1	P18421	Proteasome subunit beta type-1	26690	6.90	7/14	106/51	28%	1.48	1.29	1.07	-1.15	-1.38	Proteolysis	Cytoplasm	K.IIEARLK.M K.MYKHSNNK
636	Cwc15	Q5BJP2	Protein CWC15 homolog	26679	5.55	7/19	78/51	26%	-1.33	-1.09	-1.17	1.22	1.14	Gene regulation	Nucleus	K.EQEQKAEEER.I R.RWDDDVVFK.N
587	Pdia3	P11598	Protein disulfide-isomerase A3	57044	5.88	15/30	179/57	25%	-1.76	-1.67	-1.59	1.06	1.11	Protein folding	ER	K.YGVSGYPTLK.I K.FVMQEEFSR.D
747	Pdia6	Q63081	Protein disulfide-isomerase A6	48542	5.00	12/31	129/57	27%	-1.69	-1.23	-1.16	1.37	1.45	Protein folding	ER	K.LAAVDATVNQVLASR.Y K.GESPVDYDGGR.T
575	Pkm2	P11980	Pyruvate kinase isozymes M1/M2	58294	6.63	10/33	83/57	15%	-1.43	-1.24	-1.25	1.15	1.15	Catabolism	Cytoplasm	K.AADVHEVR.K R.AATESFASDPILYRPVAVALDTK.G
670	Gdi1	P50398	Rab GDP dissociation inhibitor alpha	51074	5.00	6/25	67/51	20%	-1.37	-1.06	-1.19	1.3	1.16	Signal transduction	Cytoplasm	K.VPSTETEALASNLMGMFEKR.R R.TDDYLDQPCLETINR.I
274	Gucy2f	P51842	Retinal guanylyl cyclase 2	125244	6.72	8/16	68/51	5%	-1.51	-1	-1.05	1.51	1.44	Biosynthesis	Plasma membrane	R.SIQKALQQIR.Q K.ENGQASAASLTR.H
478	Arhgap29	Q5PQJ5	Rho GTPase-activating protein 29	143394	6.57	10/22	64/57	9%	1.04	1.25	1.39	1.2	1.34	Signal transduction	Cytoplasm	R.NDLENTK.R K.LQGKMHIFGAEFIQVAK.K
914	Slmap	P0C219	Sarcolemmal membrane-associated protein	99018	5.14	7/19	62/51	7%	-1.36	-1.27	-1.34	1.07	1.02	Cytoskeleton regulation	Plasma membrane	R.CQQCEVQQR.E K.EWDVLENECR.S
704	Scrn1	Q6AY84	Secernin-1	46994	4.73	6/16	88/51	15%	1.12	-1.05	-1.49	-1.18	-1.67	Exocytosis	Cytoplasm	K.VECTYISIDQVPR.T R.DEAWVLETVGK.Y
719	Sept11	B3GNI6	Septin-11	50005	6.24	13/43	92/51	26%	-1.61	-1.38	-1.19	1.16	1.34	Cell growth	Cytoplasm	K.FESDPATHNEPGVR.L R.SYELQESNVR.L
910	Sept2	Q91Y81	Septin-2	41737	6.15	6/19	62/51	14%	-1.76	-1.49	-1.46	1.18	1.21	Cell growth	Cytoplasm	R.LTVVDTPGYGDAINSR.D K.TIISYIDEQFER.Y
1131	Ppp1ca	P62138	Serine/threonine-protein phosphatase PP1-alpha catalytic subunit	38229	5.94	6/14	82/57	18%	-1.29	1.16	1.12	1.49	1.44	Signal transduction	Cytoplasm	K.LNLDSIIGR.L R.LLEVQGSRPGK.N
764	Serpinh1	P29457	Serpin H1	46602	8.88	15/42	121/57	26%	-1.92	1.42	-1.28	2.73	1.51	Protein folding	ER	R.EQFVEFR.D K.DWILPSDYDHAEAEAR.H
783	Serpinh1	P29457	Serpin H1	46602	8.88	6/19	93/57	18%	-1.98	-1.57	-1.16	1.26	1.71	Protein folding	ER	K.HLAGLGLTEAIDK.N R.DNQSGSLLFIGR.L
819	Serpinh1	P29457	Serpin H1	46602	8.88	11/32	76/57	22%	-1.72	-1.35	-1.2	1.27	1.44	Protein folding	ER	K.TIIQNPTDQQK.K R.AFFSEVER.R
822	Serpinh1	P29457	Serpin H1	46602	8.88	13/35	108/51	32%	-1.89	-1.66	-1.43	1.14	1.33	Protein folding	ER	R.LYGPSSVSFADDFVR.S R.SALQSINEWASQTTDGK.L
1257	Esd	B0BNE5	S-formylglutathione hydrolase	31971	6.44	8/36	80/57	25%	-1.34	1.15	-1.18	1.55	1.13	Metabolism	Cytoplasm	K.SGCQQAASEHGLVVIAPDTSPR.G K.KAFNGYLGPDQSK.W

1300	Stam2	Q5XHY7	Signal transducing adapter molecule 2	57579	4.88	6/19	58/51	10%	-1.42	-1.28	-1.33	1.1	1.07	Signal transduction	Cytoplasm	R.LADALQELR.A R.NSNLVGAAHEELQQSR.I
978	Sord	P27867	Sorbitol dehydrogenase	38780	7.14	8/15	137/57	24%	-1.46	1.08	-1.05	1.58	1.39	Metabolism	Mitochondrion	R.VMGLGLSPEEK.Q R.AIASATEGGSVPQIR.A
527	Stip1	O35814	Stress-induced-phosphoprotein 1	63158	6.40	7/11	71/57	10%	-1.56	-1.28	-1.23	1.21	1.27	Protein folding	Cytoplasm	K.LDPQNHVLYSNR.S R.KAAALEFLNR.F
548	Stip1	O35814	Stress-induced-phosphoprotein 1	63158	6.40	9/18	109/57	14%	-1.66	-1.37	-1.3	1.21	1.27	Protein folding	Cytoplasm	K.AAALEFLNR.F R.TLLSDPTYR.E
1534	Sod1	P07632	Superoxide dismutase [Cu-Zn]	16073	5.88	7/49	91/57	40%	-1.58	-1.36	-1.54	1.16	1.02	Redox regulation	Cytoplasm	R.SYELQESNVR.L K.LTIVDTVGFGDQINK.D
574	Tcp1	P28480	T-complex protein 1 subunit alpha	60835	5.86	9/34	81/51	12%	-1.42	-1.01	-1.19	1.4	1.19	Protein folding	Cytoplasm	K.SSLGPVGLDK.M R.YPVNSVNILK.A
591	Cct2	Q5XIM9	T-complex protein 1 subunit beta	57764	6.01	15/28	161/57	22%	-1.77	-1.28	-1.37	1.38	1.29	Protein folding	Cytoplasm	K.AGADEERAETAR.L K.ILLSSGR.D
1184	Cct2	Q5XIM9	T-complex protein 1 subunit beta	57764	6.01	6/18	75/51	12%	-1.71	-1.36	-1.28	1.25	1.33	Protein folding	Cytoplasm	K.ILIANTGMDTDK.I K.LIEEVMIGEDK.L
571	Cct4	Q7TPB1	T-complex protein 1 subunit delta	58576	8.24	12/43	101/57	22%	-1.48	-1.16	-1.01	1.27	1.47	Protein folding	Cytoplasm	K.LGGTIDDCELVEGLVLTQK.V K.VANSGITR.V
516	Cct5	Q68FQ0	T-complex protein 1 subunit epsilon	59955	5.51	20/53	186/57	30%	-1.88	-1.2	-1.35	1.56	1.39	Protein folding	Cytoplasm	K.FSIEDLKAQPK.Q R.NYQARNFLR.A
157	Vcp	P46462	Transitional endoplasmic reticulum ATPase	89977	5.14	13/17	143/51	13%	-1.49	-1.06	-1.26	1.42	1.19	Vesicle trafficking	Cytoplasm	R.GILLYGPPGTGK.T
1454	Tpt1	P63029	Translationally-controlled tumor protein	19564	4.76	6/20	75/51	30%	-1.53	-1.37	-1.28	1.12	1.2	Cell growth	Cytoplasm	R.DLISHDELFSDIYK.I K.LEEQKPER.V
688	Tpm3	Q63610	Tropomyosin alpha-3 chain	29217	4.75	7/15	81/51	24%	-2.22	-1.34	-1.22	1.66	1.82	Cytoskeleton	Cytoplasm	K.MELQEIQLKEAK.H R.TEERAELAESR.C
530	Tpm2	P58775	Tropomyosin beta chain	32931	4.66	8/29	73/51	23%	-1.44	-1.02	-1.27	1.41	1.13	Cytoskeleton	Cytoplasm	R.SEERAEVAESK.C K.SLEAQADKYSTK.E
731	Tubb5	P69897	Tubulin beta-5 chain	50095	4.78	6/20	59/51	10%	-1.53	-1.13	-1.2	1.36	1.28	Cytoskeleton	Cytoplasm	R.FPGQLNADLR.K K.LAVNMVPFPR.L
746	Tubb5	P69897	Tubulin beta-5 chain	50095	4.78	10/34	107/51	23%	-1.97	-1.23	-1.29	1.61	1.53	Cytoskeleton	Cytoplasm	R.YLTVAAVFR.G K.NSSYFVEWIPNNVK.T
1576	Tubb5	P69897	Tubulin beta-5 chain	50095	4.78	10/49	89/51	20%	-2.02	1.18	1.27	-1.71	-1.59	Cytoskeleton	Cytoplasm	R.FPGQLNADLR.K K.LAVNMVPFPR.L
572	Yars	Q4KM49	Tyrosyl-tRNA synthetase, cytoplasmic	59420	6.57	7/18	82/51	11%	-1.7	-1.22	-1.29	1.39	1.31	Biosynthesis	Cytoplasm	K.EYTLDVYR.L K.VDAQFGGIDQR.K
1418	Coq7	Q63619	Ubiquinone biosynthesis protein COQ7 homolog (Fragment)	20241	5.64	6/24	75/57	34%	1.17	1.54	-1.28	1.31	-1.5	Biosynthesis	Mitochondrion	K.FNELMVAFR.V R.MLMEEDAEKYEELLQVIK.Q
1038	C3orf26	Q5FVR6	Uncharacterized protein C3orf26 homolog	31824	8.96	7/22	75/51	19%	-1.34	-1.22	-1.07	1.1	1.25	Gene regulation	Nucleus	K.DTVPVPEKTK.Q K.LIKGHYSSSR.S
429	Vps33a	Q63615	Vacuolar protein sorting-associated protein 33A	67870	6.60	7/21	58/51	10%	-1.58	1.3	-1.15	2.05	1.37	Vesicle trafficking	Endosome	R.VNLNVLR.E R.ILPGPHFEER.Q
665	Vim	P31000	Vimentin	53757	5.06	6/13	80/51	12%	1.66	-1.38	1.17	-2.29	-1.42	Cytoskeleton	Cytoplasm	R.SLYSSSPGGAYVTR.S K.VELQELNDR.F

695	Vim	P31000	Vimentin	53757	5.06	7/23	81/51	15%	-1.72	-1.29	1.01	1.34	1.74	Cytoskeleton	Cytoplasm	R.SYVTTSTR.T R.SLYSSSPGGAYVTR.S
842	Vim	P31000	Vimentin	53757	5.06	22/57	141/51	37%	1.82	1.16	-1.36	-1.58	-2.47	Cytoskeleton	Cytoplasm	R.EYQDLLNVK.M K.MALDIEIATYR.K
861	Vim	P31000	Vimentin	53757	5.06	8/34	77/57	16%	1.58	1.36	-1.22	-1.16	-1.94	Cytoskeleton	Cytoplasm	K.GVLLFGPPGTGK.T R.AVANRTDACFIR.V
1615	Vim	P31000	Vimentin	53757	5.06	16/58	93/51	29%	-1.55	-1.32	-1.12	1.18	1.39	Cytoskeleton	Cytoplasm	K.GTNESLER.Q R.EMEENFALEAANYQDTIGR.L
431	Wdr1	Q5RKI0	WD repeat-containing protein 1	66824	6.15	7/10	102/51	8%	-1.36	-1	-1.1	1.36	1.24	Cytoskeleton regulation	Cytoplasm	R.IAVVGEGR.E K.FTIGDHSR.F

heart ischemia–reperfusion injury. Accordingly, H9C2 cells were used to examine protein activity changes in PI3K pathway and migration-associated cytoskeletal proteins during ROS and HMW-HA treatments (Fig. 7). Immunoblotting analysis indicated that the serine 473 phosphorylation of Akt was significantly decreased during H_2O_2-treatment; however, the phosphorylation of Akt was restored when the H9C2 cells were pre-treated with 0.3% HMW-HA for 30 min. Additionally, migration-associated proteins, Src kinase and FAK, were both dephosphorylated during H_2O_2-treatment but recovered when the cardiomyocytes were pre-treated with HMW-HA for 30 min. In summary, ROS-induced ischemia–reperfusion injury in cardiomyocytes are significantly relieved by HMW-HA in both cell survival and wound healing repair.

4. Discussion

Ischemia–reperfusion injury is one of the major myocardial damages causing death in both men and women worldwide. The injury includes repeatedly limiting blood supply and inducing tissue inflammation. Thus, ischemia–reperfusion eventually damages heart tissue enough to cause a wound. Recent studies also showed that ROS are major players in this disease (Venardos and Kaye, 2007; Zhao, 2004; Saini et al., 2004) and Src kinase inhibition and ROS scavengers contribute to the alleviation of this disease (Hwang et al., 2008; Pasdois et al., 2007; Chen and Chow, 2005; Chou et al., 2010). Moreover, researchers found that plant extracts such as polyphenols are widely used against heart ischemia–reperfusion injury (Yanagi et al., 2011). However, these substances largely function in the remove of ROS only, but seldom reported to repair wound tissues. In this study, since HA has been reported to potentially neutralize ROS as well as promote wound healing (Yang et al., 2010; Nakamura et al., 1997; Pauloin et al., 2009a), we thus investigate whether these HA properties can apply to heart ischemia–reperfusion injury. The results firmly indicated HA can promote wound curing, cell migration and dramatically reduce H_2O_2-induced cell death in cardiomyocytes, yet the role of various forms of HA on mechanisms of cardiomyocyte repairing process following heart ischemia–reperfusion has not been known. Accordingly, we further concentrated on the correlation between the molecular weight property of HA and its capacity against H_2O_2-induced cardiomyocyte damages. Results showed that only HMW-HA was able to reduce H_2O_2-induced toxic effects and recover H_2O_2-induced impairments in wound healing. By means of proteomic analysis, HMW-HA was found to dominantly stimulate the expression of cytoskeleton/cytoskeleton-regulatory proteins, folding-associated proteins and biosynthesis-related proteins after encountering H_2O_2-damage.

Cytoskeleton/cytoskeleton regulation proteins including actin, cytokeratin 10, myosin light polypeptide 6, myosin regulatory light chain 12B, peripherin, tropomyosin, tubulin, myosin, vimentin, echinoderm microtubule-associated protein, ezrin, fascin, WD repeat-containing protein 1 were significantly impaired by ROS treatment but rescued by HMW-HA. For example, ezrin, an intermediate between the plasma membrane and the actin cytoskeleton, plays a key role in cell surface structure adhesion, migration, and organization. Fascin, a beta-catenin binding protein, localizes at the leading edges and borders of epithelial and endothelial cells. Fascin functions in regulating cytoskeletal organization for the maintenance of cell adhesion, coordinating invasion and motility. Impaired fascin expression or function has been implicated in numerous cancers (Grothey et al., 2000; Vignjevic et al., 2007). These cytoskeleton/cytoskeleton regulation proteins were dominantly down-regulated during H_2O_2 treatment but significant recovery under pre-treated with HMW-HA implying that the expression of these proteins are modulated by HMW-HA.

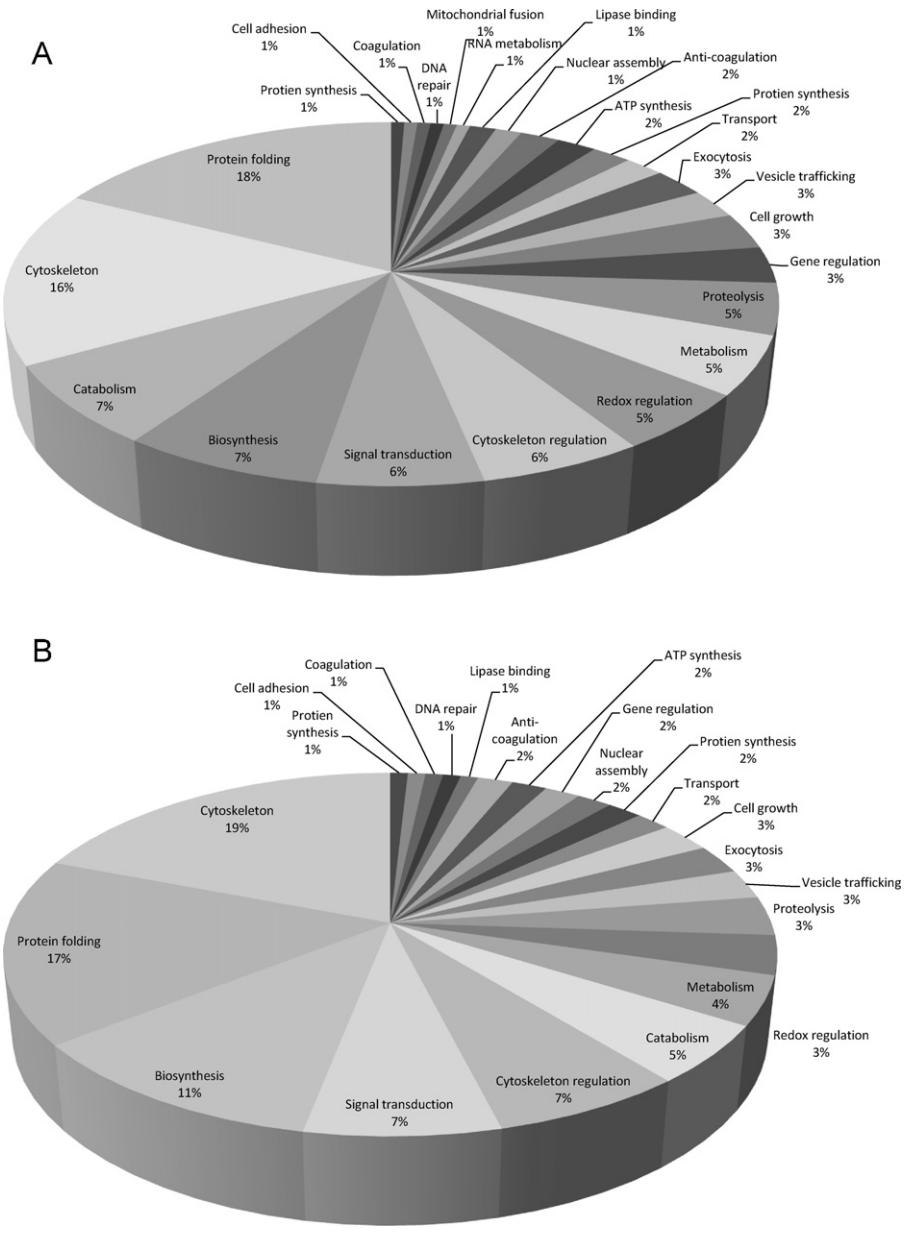

Fig. 5. Functional classification of differentially expressed proteins from H_2O_2-treated (A) and high molecular weight hyaluronic acid treated (B) cardiomyocyte H9C2.

The proteins responsible for protein folding (such as heat shock cognate 71 kDa protein) were identified in our present proteomic study. Heat shock protein 71 protein is a molecular chaperone that accelerates the cell recovery from harmful conditions by reducing the concentrations of unfolded or denatured proteins (Rohde et al., 2005). Our proteomic study showed that heat shock 71 kDa protein was down-regulated in H_2O_2-treated H9C2 cells but its expression level was increased after HMW-HA treatment. This demonstrates H_2O_2 indeed triggers the cellular stress in H9C2 cells while HMW-HA has ability to release the ROS-induced cellular stress. Hence, the expression of heat shock 71 kDa protein was up-regulated as control cells.

Importantly, our data also indicated that HA might modulate the activation levels of pAkt, pSrc and pFAK which are essential for maintaining cell survival, cell motility and cytoskeleton rearrangement. We have revealed H_2O_2 induced a reduced phosphorylation of Akt pS473, Src pY416 and FAK pY576/577; these changes were reversed when incubating H9C2 cardiomyocytes with 0.3% HMW-HA, thereby implying HA might not only contribute cardiomyocyte wound healing via reported CD44/PKC/FAK pathway (Kim et al., 2008), also activation of PI3 kinase pathway to promote cell viability.

HA has been described to specifically interact with CD44 receptor on plasma membrane (Toole, 2004) and the receptor has also been reported to express on the surface of cardiomyocytes (Hellstrom et al., 2006), suggesting that HA is strongly binding to plasma membrane via CD44 receptor and play roles to maintain the plasma membrane integrity of cardiomyocytes during ROS-damage. In addition to molecular size, our studies revealed that the concentration of HA is important to provide protection against the toxic effect of H_2O_2. Our study showed that 0.3% of HMW-HA is the optimal concentration to protect cardiomyocytes from H_2O_2 damage and induce cell proliferation in advanced. At this optimal concentration, HMW-HA might form an appropriate biopolymer structure that covers the outer surface of plasma membrane via linking with CD44 receptors. The CD44 receptor bound HA might consequently stimulate cell proliferation (Wang et al., 2011) as well as mask the death receptors from activation to maintain cell

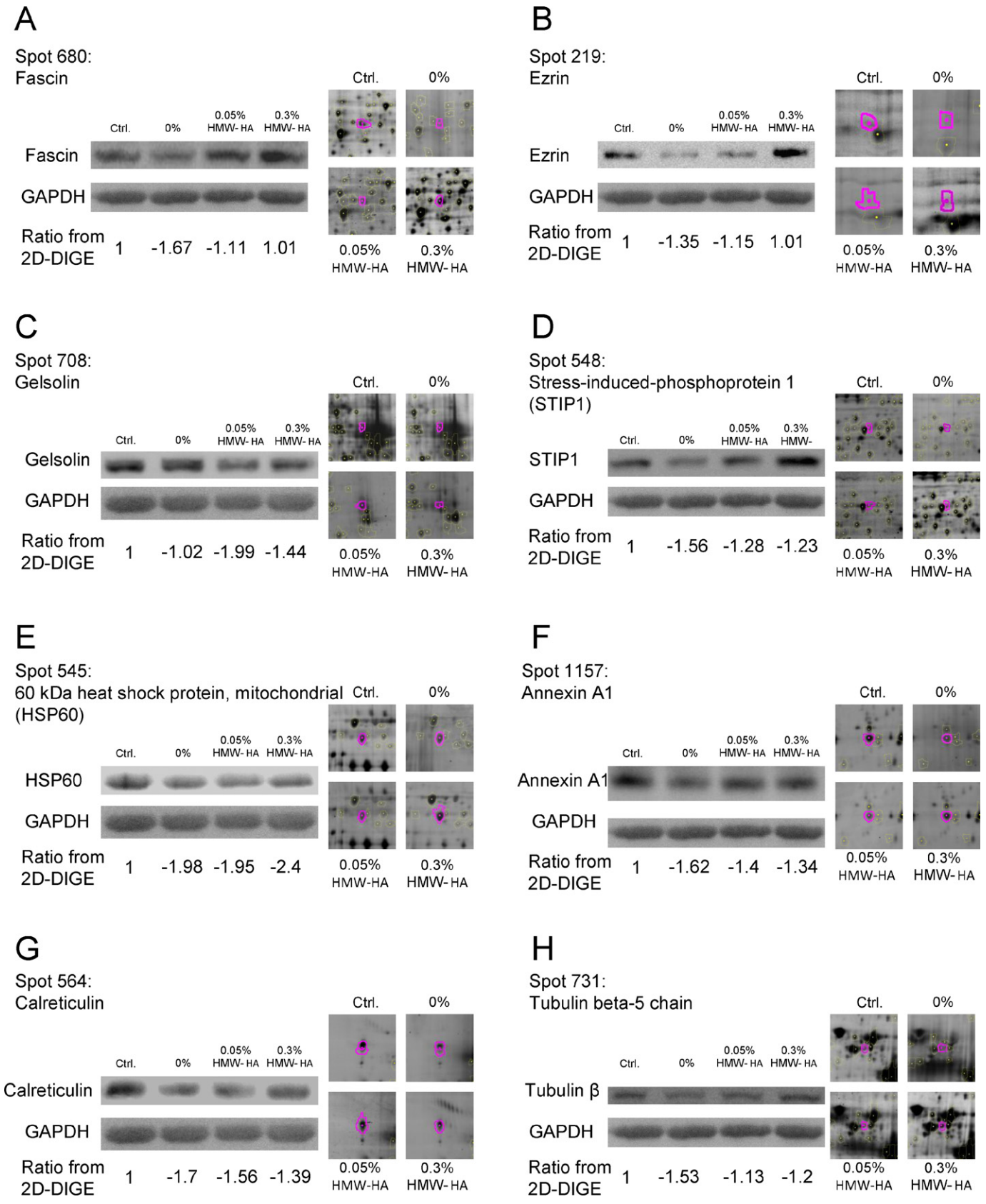

Fig. 6. Validation of expression proteomic results in H_2O_2-treated H9C2 cells with pre-treated by HMW-HA by immunoblotting. The altered expression of identified proteins: (A) fascin, (B) ezrin, (C) gelsolin, (D) stress-induced-phosphoprotein 1, (E) 60 kDa heat shock protein, mitochondrial, (F) annexin A1 and (G) calreticulin, (H) tubulin beta-5 chain were assessed by immunoblotting (left panels). The protein 2D-DIGE maps are also shown in right panels.

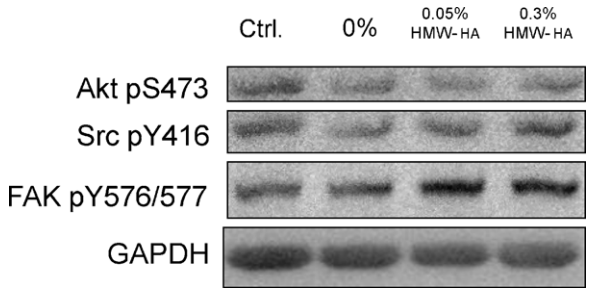

Fig. 7. Effect of HMW-HA on H_2O_2-induced signaling events and phosphorylated protein recovery. Total cell lysates (TCL) prepared from untreated and H_2O_2-/HMW-HA-treated H9C2 cells were immunoblotted with antibodies against the phosphorylated serine residue 473 on Akt protein, the phosphorylated tyrosine residue 416 on Src protein, the phosphorylated tyrosine residue 576/577 on FAK protein and loading control, GAPDH. Cells were left untreated or pre-treated with 0.05% HMW-HA/0.3% HMW-HA for 30 min followed by treated with 400 μM H_2O_2 for 24 h.

survival and function (Pauloin et al., 2009b). However, the cell viability and protection property has been dramatically dropped down while the concentration of HMW-HA was higher than 0.5% (data not shown), implying high concentrations of HMW-HA might interfere metabolism, nutrients and gas exchanges. This hypothesis has also been described by Miyauchi et al. who provided evidence to show higher concentrations of HAs are much more viscous than culture medium that they inhibit epithelial migration and the diffusion of nutrients and cell metabolism (Miyauchi et al., 1990).

In conclusion, the present study showed that both HMW-HA (1000 kDa) and LMW-HA (100 kDa) do not have obvious toxic effect on rat cardiomyocytes, H9C2. However, only HMW-HA significantly reduces the H_2O_2-induced cytotoxic effects in cardiomyocytes and increases wound healing ability at the same time. Thus, the current study is an appropriate research for prospect clinical practice. In future, researchers might design a tissue-specific targeting strategy to transport HMW-HA into heart ischemia site to alleviate the disease as well as increase plasma HMW-HA concentration in heart ischemia patients by intravenous injection. To sum up, the finding of this study might be applied in heart ischemia–reperfusion injury therapy to repair the ROS-damage of cardiomyocytes and might be used to design biomaterials to accelerate heart wound healing.

Conflicts of interest

The authors confirm that there are no conflicts of interest.

Acknowledgements

This work was supported by NSC grant (100-2311-B-007-005 and 101-2311-B-007-011) from National Science Council, Taiwan, NTHU and CGH grant (100N2723E1) from National Tsing Hua University, NTHU Booster grant (99N2908E1) from National Tsing Hua University, Toward World-Class University project from National Tsing Hua University (100N2051E1) and VGHUST grant (99-P5-22) from Veteran General Hospitals University System of Taiwan.

References

Barrett, W.C., DeGnore, J.P., Keng, Y.F., Zhang, Z.Y., Yim, M.B., Chock, P.B., 1999. Roles of superoxide radical anion in signal transduction mediated by reversible regulation of protein-tyrosine phosphatase 1B. J. Biol. Chem. 274, 34543–34546.

Chan, H.L., Gaffney, P.R., Waterfield, M.D., Anderle, H., Peter, M.H., Schwarz, H.P., Turecek, P.L., Timms, J.F., 2006. Proteomic analysis of UVC irradiation-induced damage of plasma proteins: serum amyloid P component as a major target of photolysis. FEBS Lett. 580, 3229–3236.

Chan, H.L., Gharbi, S., Gaffney, P.R., Cramer, R., Waterfield, M.D., Timms, J.F., 2005. Proteomic analysis of redox- and ErbB2-dependent changes in mammary luminal epithelial cells using cysteine- and lysine-labelling two-dimensional difference gel electrophoresis. Proteomics 5, 2908–2926.

Chen, J.K., Chow, S.E., 2005. Antioxidants and myocardial ischemia: reperfusion injuries. Chang Gung Med. J. 28, 369–377.

Chen, Y.W., Chou, H.C., Lyu, P.C., Yin, H.S., Huang, F.L., Chang, W.S., Fan, C.Y., Tu, I.F., Lai, T.C., Lin, S.T., Lu, Y.C., Wu, C.L., Huang, S.H., Chan, H.L., 2011a. Mitochondrial proteomics analysis of tumorigenic and metastatic breast cancer markers. Funct. Integr. Genomics 11, 225–239.

Chen, Y.W., Liu, J.Y., Lin, S.T., Li, J.M., Huang, S.H., Chen, J.Y., Wu, J.Y., Kuo, C.C., Wu, C.L., Lu, Y.C., Chen, Y.H., Fan, C.Y., Huang, P.C., Law, C.H., Lyu, P.C., Chou, H.C., Chan, H.L., 2011b. Proteomic analysis of gemcitabine-induced drug resistance in pancreatic cancer cells. Mol. Biosyst. 7, 3065–3074.

Chou, H.C., Chen, Y.W., Lee, T.R., Wu, F.S., Chan, H.T., Lyu, P.C., Timms, J.F., Chan, H.L., 2010. Proteomics study of oxidative stress and Src kinase inhibition in H9C2 cardiomyocytes: a cell model of heart ischemia reperfusion injury and treatment. Free Radic. Biol. Med. 49, 96–108.

Chou, H.C., Lu, Y.C., Cheng, C.S., Chen, Y.W., Lyu, P.C., Lin, C.W., Timms, J.F., Chan, H.L., 2012. Proteomic and redox-proteomic analysis of berberine-induced cytotoxicity in breast cancer cells. J. Proteomics 75, 3158–3176.

D'Autreaux, B., Toledano, M.B., 2007. ROS as signalling molecules: mechanisms that generate specificity in ROS homeostasis. Nat. Rev. Mol. Cell Biol. 8, 813–824.

Ferrari, R., Ceconi, C., Curello, S., Cargnoni, A., Pasini, E., De Giuli, F., Albertini, A., 1991. Role of oxygen free radicals in ischemic and reperfused myocardium. Am. J. Clin. Nutr. 53, 215S–222S.

Finkel, T., 2000. Redox-dependent signal transduction. FEBS Lett. 476, 52–54.

Grothey, A., Hashizume, R., Sahin, A.A., McCrea, P.D., 2000. Fascin, an actin-bundling protein associated with cell motility, is upregulated in hormone receptor negative breast cancer. Br. J. Cancer 83, 870–873.

Hellstrom, M., Johansson, B., Engstrom-Laurent, A., 2006. Hyaluronan and its receptor CD44 in the heart of newborn and adult rats. Anat. Rec. A Discov. Mol. Cell Evol. Biol. 288, 587–592.

Huang, H.L., Hsing, H.W., Lai, T.C., Chen, Y.W., Lee, T.R., Chan, H.T., Lyu, P.C., Wu, C.L., Lu, Y.C., Lin, S.T., Lin, C.W., Lai, C.H., Chang, H.T., Chou, H.C., Chan, H.L., 2010. Trypsin-induced proteome alteration during cell subculture in mammalian cells. J. Biomed. Sci. 17, 36.

Hung, P.H., Chen, Y.W., Cheng, K.C., Chou, H.C., Lyu, P.C., Lu, Y.C., Lee, Y.R., Wu, C.T., Chan, H.L., 2011. Plasma proteomic analysis of the critical limb ischemia markers in diabetic patients with hemodialysis. Mol. Biosyst. 7, 1990–1998.

Hwang, J.T., Kwon, D.Y., Park, O.J., Kim, M.S., 2008. Resveratrol protects ROS-induced cell death by activating AMPK in H9c2 cardiac muscle cells. Genes Nutr. 2, 323–326.

Kim, Y., Lee, Y.S., Choe, J., Lee, H., Kim, Y.M., Jeoung, D., 2008. CD44-epidermal growth factor receptor interaction mediates hyaluronic acid-promoted cell motility by activating protein kinase C signaling involving Akt, Rac1, Phox, reactive oxygen species, focal adhesion kinase, and MMP-2. J. Biol. Chem. 283, 22513–22528.

Kwon, J., Lee, S.R., Yang, K.S., Ahn, Y., Kim, Y.J., Stadtman, E.R., Rhee, S.G., 2004. Reversible oxidation and inactivation of the tumor suppressor PTEN in cells stimulated with peptide growth factors. Proc. Natl. Acad. Sci. U.S.A. 101, 16419–16424.

Lai, T.C., Chou, H.C., Chen, Y.W., Lee, T.R., Chan, H.T., Shen, H.H., Lee, W.T., Lin, S.T., Lu, Y.C., Wu, C.L., Chan, H.L., 2010. Secretomic and proteomic analysis of potential breast cancer markers by two-dimensional differential gel electrophoresis. J. Proteome Res. 9, 1302–1322.

Lin, C.P., Chen, Y.W., Liu, W.H., Chou, H.C., Chang, Y.P., Lin, S.T., Li, J.M., Jian, S.F., Lee, Y.R., Chan, H.L., 2011. Proteomic identification of plasma biomarkers in uterine leiomyoma. Mol. Biosyst.

Martin, J., Lutter, G., Sarai, K., Senn-Grossberger, M., Takahashi, N., Bitu-Moreno, J., Haberstroh, J., Beyersdorf, F., 2001. Investigations on the new free radical scavenger polynitroxyl-albumin to prevent ischemia and reperfusion injury after orthotopic heart transplantation in the pig model. Eur. J. Cardiothorac. Surg. 19, 321–325.

McCord, J.M., 1974. Free radicals and inflammation: protection of synovial fluid by superoxide dismutase. Science 185, 529–531.

Miyauchi, S., Sugiyama, T., Machida, A., Sekiguchi, T., Miyazaki, K., Tokuyasu, K., Nakazawa, K., 1990. The effect of sodium hyaluronate on the migration of rabbit corneal epithelium. I. An in vitro study. J. Ocul. Pharmacol. 6, 91–99.

Nakamura, M., Sato, N., Chikama, T.I., Hasegawa, Y., Nishida, T., 1997. Hyaluronan facilitates corneal epithelial wound healing in diabetic rats. Exp. Eye Res. 64, 1043–1050.

Pasdois, P., Quinlan, C.L., Rissa, A., Tariosse, L., Vinassa, B., Costa, A.D., Pierre, S.V., Dos, S.P., Garlid, K.D., 2007. Ouabain protects rat hearts against ischemia–reperfusion injury via pathway involving src kinase, mitoKATP, and ROS. Am. J. Physiol. Heart Circ. Physiol. 292, H1470–H1478.

Pauloin, T., Dutot, M., Joly, F., Warnet, J.M., Rat, P., 2009a. High molecular weight hyaluronan decreases UVB-induced apoptosis and inflammation in human epithelial corneal cells. Mol. Vis. 15, 577–583.

Pauloin, T., Dutot, M., Liang, H., Chavinier, E., Warnet, J.M., Rat, P., 2009b. Corneal protection with high-molecular-weight hyaluronan against in vitro and in vivo sodium lauryl sulfate-induced toxic effects. Cornea 28, 1032–1041.

Pauloin, T., Dutot, M., Warnet, J.M., Rat, P., 2008. In vitro modulation of preservative toxicity: high molecular weight hyaluronan decreases apoptosis and oxidative stress induced by benzalkonium chloride. Eur. J. Pharm. Sci. 34, 263–273.

Pucheu, S., Boucher, F., Sulpice, T., Tresallet, N., Bonhomme, Y., Malfroy, B., de Leiris, J., 1996. EUK-8 a synthetic catalytic scavenger of reactive oxygen species protects isolated iron-overloaded rat heart from functional and structural damage induced by ischemia/reperfusion. Cardiovasc. Drugs Ther. 10, 331–339.

Rhee, S.G., Chang, T.S., Bae, Y.S., Lee, S.R., Kang, S.W., 2003. Cellular regulation by hydrogen peroxide. J. Am. Soc. Nephrol. 14, S211–S215.
Rhee, S.G., Kang, S.W., Jeong, W., Chang, T.S., Yang, K.S., Woo, H.A., 2005. Intracellular messenger function of hydrogen peroxide and its regulation by peroxiredoxins. Curr. Opin. Cell Biol. 17, 183–189.
Rohde, M., Daugaard, M., Jensen, M.H., Helin, K., Nylandsted, J., Jaattela, M., 2005. Members of the heat-shock protein 70 family promote cancer cell growth by distinct mechanisms 2. Genes Dev. 19, 570–582.
Ross, S.H., Lindsay, Y., Safrany, S.T., Lorenzo, O., Villa, F., Toth, R., Clague, M.J., Downes, C.P., Leslie, N.R., 2007. Differential redox regulation within the PTP superfamily. Cell Signal. 19, 1521–1530.
Saini, H.K., Machackova, J., Dhalla, N.S., 2004. Role of reactive oxygen species in ischemic preconditioning of subcellular organelles in the heart. Antioxid. Redox. Signal. 6, 393–404.
Scandalios, J.G., 2002. The rise of ROS. Trends Biochem. Sci. 27, 483–486.
Takano, H., Zou, Y., Hasegawa, H., Akazawa, H., Nagai, T., Komuro, I., 2003. Oxidative stress-induced signal transduction pathways in cardiac myocytes: involvement of ROS in heart diseases. Antioxid. Redox. Signal. 5, 789–794.
Timms, J.F., Cramer, R., 2008. Difference gel electrophoresis. Proteomics 8, 4886–4897.
Toole, B.P., 2004. Hyaluronan: from extracellular glue to pericellular cue. Nat. Rev. Cancer 4, 528–539.
Venardos, K.M., Kaye, D.M., 2007. Myocardial ischemia–reperfusion injury, antioxidant enzyme systems, and selenium: a review. Curr. Med. Chem. 14, 1539–1549.
Vignjevic, D., Schoumacher, M., Gavert, N., Janssen, K.P., Jih, G., Lae, M., Louvard, D., Ben Ze'ev, A., Robine, S., 2007. Fascin, a novel target of beta-catenin-TCF signaling, is expressed at the invasive front of human colon cancer. Cancer Res. 67, 6844–6853.
Wang, Y.Z., Cao, M.L., Liu, Y.W., He, Y.Q., Yang, C.X., Gao, F., 2011. CD44 mediates oligosaccharides of hyaluronan-induced proliferation, tube formation and signal transduction in endothelial cells. Exp. Biol. Med. (Maywood) 236, 84–90.
Wu, C.L., Chou, H.C., Cheng, C.S., Li, J.M., Lin, S.T., Chen, Y.W., Chan, H.L., 2012. Proteomic analysis of UVB-induced protein expression- and redox-dependent changes in skin fibroblasts using lysine- and cysteine-labeling two-dimensional difference gel electrophoresis. J. Proteomics 75, 1991–2014.
Yanagi, S., Matsumura, K., Marui, A., Morishima, M., Hyon, S.H., Ikeda, T., Sakata, R., 2011. Oral pretreatment with a green tea polyphenol for cardioprotection against ischemia–reperfusion injury in an isolated rat heart model. J. Thorac. Cardiovasc. Surg. 141, 511–517.
Yang, G., Espandar, L., Mamalis, N., Prestwich, G.D., 2010. A cross-linked hyaluronan gel accelerates healing of corneal epithelial abrasion and alkali burn injuries in rabbits. Vet. Ophthalmol. 13, 144–150.
Young, I.S., Woodside, J.V., 2001. Antioxidants in health and disease. J. Clin. Pathol. 54, 176–186.
Zhao, Z.Q., 2004. Oxidative stress-elicited myocardial apoptosis during reperfusion. Curr. Opin. Pharmacol. 4, 159–165.
Zima, A.V., Blatter, L.A., 2006. Redox regulation of cardiac calcium channels and transporters. Cardiovasc. Res. 71, 310–321.